Carbonization of Sewage Sludge and Effects of Process Conditions on Resources and Energy Recovery Potential

July 2018

YU YANG

Carbonization of Sewage Sludge and Effects of Process Conditions on Resources and Energy Recovery Potential

A Dissertation Submitted to

Graduate School of Life and Environmental Sciences,

University of Tsukuba

in Partial Fulfillment of the Requirements

for the Doctor Degree of Philosophy of Environmental Studies

(Doctoral Program in Sustainable Environmental Studies)

YU YANG

Abstract

Nowadays, the growing serious environmental issues accompanied by energy and resources exhausted are increasingly becoming the main survive crisis as human beings. As a by-product of wastewater treatment system. Sewage sludge treatment and resource and energy recovery technology are of great ongoing. In this study, hydrothermal carbonization (HTC) as an emerging method was applied to recover nutrient especially P, as well as energy from both domestic sewage sludge and industrial sludge. The main purpose of this study was to fully evaluate the nutrient recovery potential and energy yield of HTC.

In order to get a deep understand between P and minerals during HTC, the effects of minerals on P immobilization during HTC were investigated in Chapter 2. Ferric (Fe), calcium (Ca) and aluminum (Al) ions, which were used as flocculants during wastewater treatment process, were added into the sludge to probe the effects on P speciation in hydrochar and mechanisms involved during HTC. All the three kinds of metal ions demonstrated significant effects on P immobilization, among which Al was the most efficient effector, yielding 93% and 96% of P immobilization respectively at 5 and 10 mmol of Al mineral additives. Both Al and Fe rather than Ca promoted the formation of non-apatite inorganic phosphate (NAIP) and reduced the amount of apatite phosphate (AP) in the hydrochar. Whereas Ca addition made significant contributions to AP content. Moreover, results from this study indicate that Al-P is the primary existing form in the hydrochar.

In Chapter 3, struvite precipitation technology was evaluated and used for P recovery from HTC liquid products. Results showed that HTC at 200 °C for 30 min favored phosphate release achieving phosphate concentrations at 579.98 mg-P/L. During the subsequent struvite precipitation, the optimum condition for P recovery was determined at pH 9 and Mg/P molar ratio of 1, realizing P recovery of 92% from the hydrolysate in addition to struvite purity of 84%. The produced struvite was confirmed by FTIR and XRD analysis, which fulfills the related standards.

In Chapter 4, HTC of anaerobic granular sludge (AGS) was investigated at different temperatures (160 - 240 °C) regarding the distributions of C, N and P in the hydrothermal products to maximize the utilization efficiency of AGS. Elemental

composition and fuel characteristics of the hydrochar were evaluated. Results indicated that the percentages of C in hydrochar increased from 43.79% to 49.81% with the increase in HTC temperature, while N showed an opposite trend, decreasing from 9.58% to 5.49%. The higher heating value of hydrochar increased up to a maximum of 24 MJ/kg at 240 °C from 20 MJ/kg at 160 °C. However, the hydrochar yield decreased remarkably from 62% to 32%. As a result, the highest net energy output was about 6.86 MJ/kg achieved at 160 °C. Results from the van Krevelen diagram suggested that dehydration and decarboxylation reactions occurred during the HTC of AGS. In addition, the thermogravimetric analysis implied that the combustion of the produced hydrochar could be completed in two phases rather than the one phase as the raw AGS. With regard to other resources utilization, HTC was proved to be effective for AGS to immobilize and recycle phosphorus. The increase in HTC temperature exerted a limited effect on P distribution, resulting in less than 5% being released into the liquid at all tested HTC temperatures. Most of P were immobilized into the produced hydrochar where the bioavailable P fractions > 80%.

Results from this work imply that the HTC of sewage sludge could provide a novel and effective solution for a reduction in energy costs of wastewater treatment or nutrients recovery simultaneously. Nutrients in sludge were redistributed by using hydrothermal technology. A part of P was released into the hydrolysate which could be recycled by struvite precipitation. High purity struvite can be achieved from sewage sludge, which could be used as slow-release fertilizers. Meanwhile, the hydrochar produced from HTC of sewage sludge could serve different application purposes (e.g. fuel or soil amendments). This study provides an alternative method to alleviate the concerns on increased sludge production rate and the secondary pollution caused by it. Further research efforts are still necessary on the maximization of energy and/or nutrient recovery from sewage sludge by using HTC.

Keywords: Sewage sludge; Hydrothermal treatment; Phosphorus recovery; minerals; Biochar; Energy recovery

Contents

Abstract ····· i
List of Tables ····· vi
List of Figures ····· vii
Abbreviations ····· ix
Chapter 1 Introduction ····· 1
1.1 Sewage sludge production and treatment ····· 1
1.1.1 Sewage sludge production ····· 1
1.1.2 Current disposal and treatment methods for sewage sludge ····· 2
1.1.3 Nutrients recovery from sewage sludge ····· 3
1.2 Hydrothermal technology ····· 4
1.2.1 Overview ····· 4
1.2.2 Fate of phosphorus during HTT ····· 5
1.2.3 Energy recovery potential of the products ····· 5
1.3 Existed problems for current HTT of sewage sludge ····· 6
1.4 Objectives ····· 8
1.5 Novelty and structure of this research ····· 9
Chapter 2 Effects of mineral additives on P immobilization from sewage sludge using hydrothermal treatment ····· 12
2.1 Introduction ····· 12
2.2 Materials and methods ····· 12
2.2.1. Materials ····· 12
2.2.2 Hydrothermal treatment procedure ····· 12
2.2.3. Analytical methods ····· 13
2.2.4. Statistical analysis ····· 14
2.3 Results and discussion ····· 14
2.3.1 Mineral addition on phosphorus immobilization in sludge during HTT ···· 14
2.3.2 Mineral addition on phosphorus fractionation in the produced biochar ···· 15
2.3.3 Biochar characterization ····· 17
2.3.4. Other additional information about the hydrolysate produced in this work ····· 18
2.4 Summary ····· 18

Chapter 3 P and N recovery from sewage sludge using a hybrid system coupling hydrothermal pretreatment with struvite precipitation ····· 32
3.1 Introduction ····· 32
3.2 Materials and methods ····· 32
3.2.1 Sludge sample ····· 32
3.2.2 Hydrothermal treatment ····· 33
3.2.3 Struvite precipitation ····· 33
3.2.4 Analytical methods ····· 34
3.2.5 Calculation ····· 35
3.3 Results and discussion ····· 36
3.3.1 Optimization of hydrothermal temperature and residence time for P and N release ····· 36
3.3.2 Optimization of struvite precipitation ····· 38
3.3.3 Mass balance and struvite purity analysis ····· 40
3.3.4 Characterization of the precipitates by struvite precipitation from the hydrolysate ····· 41
3.4 Summary ····· 42
Chapter 4 Hydrothermal carbonization of anaerobic granular sludge: the potential application of hydrochars ····· 55
4.1 Introduction ····· 55
4.2 Materials and methods ····· 56
4.2.1 Materials ····· 56
4.2.2 Hydrothermal carbonization of AGS ····· 56
4.2.3 Hydrolysate analysis ····· 56
4.2.4 Hydrochar characterization ····· 57
4.2.5 Energy calculation ····· 57
4.3 Results and discussion ····· 58
4.3.1 Effect of HTT on organics transformation ····· 58
4.3.2 Effect of HTT on P and N ····· 59
4.3.3 Elemental composition and higher heating value of hydrochar ····· 60
4.3.4 Additional properties for the hydrochar ····· 62
4.4 Summary ····· 63
Chapter 5 Conclusions and future research ····· 76
5.1 Conclusions ····· 76

5.2. Future research ····· 77
References ····· 78
Acknowledgements ····· 84

List of Tables

Chapter 2

Table 2-1 Main physicochemical characteristics of the raw primary sludge used in the experiments 20

Table 2-2 Minerals concentration in the hydrolysate obtained from HTT of sludge after addition of different mineral additives. 21

Table 2-3 Pearson correlation coefficients between various minerals and P fractionation 22

Table 2-4 The mass balance of P in solid and hydrolysate after HTT 23

Chapter 3

Table 3-1 Main physicochemical characteristics of anaerobically digested sludge used in the experiments 44

Table 3-2 Effect of initial pH on P and NH_4-N removal from hydrolysate after $MgCl_2$ being added to a molar Mg/P ratio of 1:1 45

Table 3-3 Effect of increase in Mg/P molar ratio on P and NH_4-N removal after 1 h struvite precipitation at initial pH of 9.0 46

Table 3-4 Comparison of produced struvite purity and its component mass changes at different initial pHs 47

Table 3-5 Main metals detected in the hydrolysate of sludge after being hydrothermally treated at 200 °C for 30 min and the struvite precipitates formed in 1 h at different initial pHs 48

Chapter 4

Table 4-1 Main characteristics of raw AGS used in this study 64

Table 4-2 Carbon and phosphorus and nitrogen distributions in HTC products of AGS at various hydrothermal temperature 65

Table 4-3 Main metals detected in the raw AGS and hydrochar of AGS after being HTT at 160, 200 and 240 ºC, respectively 66

Table 4-4 A comparison between unbroken AGS and smashed AGS on nutrients release during HTT 67

Table 4-5 Proximate and ultimate analyses of hydrochar (%, TS based) 68

List of Figures

Chapter 1

Fig. 1-1. Experimental structure of this study 9

Fig. 1-2 The typical treatment process for sewage sludge produced from WWTPs 10

Fig. 1-3 Various methods for resource recovery from waste sludge 11

Chapter 2

Fig. 2-1 Effects of different mineral additives on TP and TAN concentrations in the hydrolysate 24

Fig. 2-2 Effects of different mineral additives on P speciation in sludge after HTT 26

Fig. 2-3 Effects of different mineral additives on soluble TOC concentration and pH in the hydrolysate from sewage sludge 27

Fig. 2-4 Effects of different mineral additives on VFA production from sludge after HTT at 200 ºC for 1 h 28

Fig. 2-5 FTIR spectra of Fe-10, Ca-10, Al-10 and Mix-10 29

Fig. 2-6 XRD patterns of Fe-10 (A), Ca-10 (B), Al-10 (C) and Mix-10 (D) 31

Chapter 3

Fig. 3-1 Changes in soluble TOC and final pH in sludge after being hydrothermally treated for 30 min at different temperatures 49

Fig. 3-2 Phosphate and ammonium release from sludge into the hydrolysate after hydrothermal treatment at different temperatures 50

Fig. 3-3 Effect of hydrothermal pretreatment temperature on VFAs production 51

Fig. 3-4 Effect of hydrothermal pretreatment temperature on soluble carbohydrates and proteins 52

Fig. 3-5 FTIR spectra of the struvite standard and struvite precipitates at pH 8, 9 and 10, respectively 53

Fig. 3-6 XRD patterns of the struvite standard and the precipitates formed in 30 min at pH 8, 9 and 10, respectively 54

Chapter 4

Fig.4-1 Energy and resources recovery based on the hybrid process coupling AGS wastewater treatment with HTC of AGS 69

Fig.4-2 Variations of proteins, carbohydrates and VFAs released from AGS into the hydrolysate (a), and VFAs species and pH in the hydrolysate after HTT at different temperatures 70
Fig.4-3 Changes of carbon (a), phosphorus (b) and nitrogen (c) distribution in the solid and liquid phases after HTT of AGS at different temperatures 71
Fig.4-4 Atomic H/C versus O/C ratios (van Krevelen diagram) of the raw AGS and hydrochars produced at different HTT temperatures 72
Fig.4-5 DTA/TG/DTG profiles for raw AGS and hydrochars produced at 160 ºC, 200 ºC and 240 ºC 74
Fig.4-6 FTIR spectra of hydrochars at different hydrothermal temperature 75

Abbreviations

AGS	Anaerobic granular sludge
AP	Apatite phosphorus
C	Carbon
FTIR	Fourier Transform Infrared Spectroscopy
HHVs	Higher Heating Values
HTT	Hydrothermal treatment
HTC	Hydrothermal carbonization
IP	Inorganic phosphorus
N	Nitrogen
NAIP	Non-apatite inorganic phosphorus
OP	Organic phosphorus
Ortho-P	Orthophosphate
P	Phosphorus
SEM	Scanning electron microscope
SMT	The Standards, Measurements and Testing
TOC	Total organic carbon
TN	Total nitrogen
TP	Total phosphorus
T(V)S	Total (volatile) solids
VFAs	Volatile fatty acids
WWTPs	Wastewater treatment plants

Chapter 1 Introduction

The growing serious environmental issues, including air, water and soil pollution accompanied by energy and resources exhausted is increasingly becoming a main survive crisis of human beings. The increased in world population and the development of the industry lead to an increasing amount of wastewater. As a result, a large amount of sewage sludge was produced from municipal and industrial wastewater treatment plants (WWTPs). Proper disposal of sewage sludge is the key to sustainable management of WWTPs. In the last decades, many efforts were focused on dewatering and reducing the amount of sewage sludge. Whereas, sewage sludge, which usually contains nutrients, metals, embedded energy potential, is regarded as a significant asset in recent years. And reclaiming and utilization of energy and nutrients from sewage sludge is becoming one of the critical issues for sustainable development. In the future, it could be expected that recovery and reuse of energy and valuable chemicals by using innovative technology is the major research field.

1.1 Sewage sludge production and treatment

1.1.1 Sewage sludge production

Biological-based wastewater treatment processes produce a large amount of sewage sludge. A large amount of sewage sludge generated from wastewater treatment plants (WWTPs) has posed a serious burden to the environment and human health (Singh et al., 2004). In China, there were more than 3700 WWTPs in operation by the end of 2014. More than 30 million tons (dry solids) of sewage sludge is generated each year (Xu et al., 2011), of which only 25% were treated properly (Zhang et al., 2016). Sewage sludge treatment results in very high costs.

As it is known, sewage sludge can be categorized as primary sludge from settling tank, waste activated sludge from activated sludge tank and anaerobically digested sludge according to the WWTP processes applied to the treatment units where sludges are originated (Tchobanoglous et al., 2003).

Sewage sludge is a complex mixture of microorganism and a variety of organics such as protein, oils, fecal materials and inorganics. And the detailed components change according to the change of feedwater and the operation technologies.

1.1.2 Current disposal and treatment methods for sewage sludge

Proper sewage sludge disposal or treatment methods are crucial to the sustainable management of WWTPs. Commonly, sludge handling and disposal accounts for almost 50% of the total costs of the wastewater plant (Karr & Keinath, 1978). Various researches have been done on sewage sludge treatment because the sludge is hard to dewater and multiple contaminants existed in the sludge (Tsang & Vesilind, 1990). Common disposal methods include land application, landfilling, composting and incineration.

Currently, 55% of sewage sludge is reported to be disposed by land application (Mulchandani and Westerhoff, 2016). Land use is an economic way for sewage sludge disposal due to nutrients can be provided for the plants. However, its continual use can result in the accumulation of heavy metals to levels detrimental to the environment. The U.S. Environmental Protection Agency (US EPA) set up a series of regulations for the use of sewage sludge, which aimed at limiting risks for the cumulative loading of heavy metals to the soil. As a result, sludge with contaminants and strong odor may no longer be disposed in land disposal. Alternatives to land use include but are not limited to landfilling (30%) (Peccia and Westerhoff, 2015). Disposing sewage sludge to landfills is considered a beneficial use only when methane recovery was included. It is estimated that about 65% of the sewage sludge in China was disposed in landfill (Wang et al., 2009). However, there is limited land for landfills and the leachate from filling sites is very difficult to treat and this situation could always last for years.

For sewage sludge treatment, it usually consists of thickening, dewatering and several main treatment technologies, including composting, anaerobic digestion and thermal treatment. In recent years, a series of thermal processes have been developed for sewage sludge utilization, including incineration, pyrolysis, gasification, wet oxidation and hydrothermal treatment. The principal goal of thermal processing of sewage sludge is the utilization of the stored energy in sludge and the minimization of environmental impacts at the same time. Incineration and co-incineration of sewage sludge are applied on a large scale. The toxic organics are destructed and the heavy metals are immobilized in the ash during these processes (Khiari et al., 2004). However, the energy efficiency of sewage sludge incineration depends upon the degree of dewatering. And one of the major concern of incineration is about harmful gas emissions. Inappropriate disposal of sewage sludge may bring secondary pollution issues like greenhouse gases (GHGs) emission and groundwater contamination (Giusti, 2009).

Conventionally, sewage sludge treatments were focused on reducing the weight and volume of sewage sludge and reducing the potential health risks. However, it is worthwhile to consider shifting the viewpoint from waste treatment toward resource and energy recovery.

1.1.3 Nutrients recovery from sewage sludge

Phosphorus and nitrogen are the main nutrients in sewage sludge. It is estimated that 16% of the total phosphorus is digested by humans and discharged into the waste stream (Rittmann et al., 2011). And recovery of phosphorus from sewage sludge posed a sustainable way for the limited resources. Nitrogen is another main nutrient in sewage sludge, mainly existed as ammonium (40%), organic nitrogen (60%) and nitrate nitrogen (1%) (Mulchandani & Westerhoff, 2016). As an indispensable element for the plant, a large number of nitrogen fertilizers were consumed every year. Excess nitrogen in water body is the primary cause of eutrophication. And recovery of nitrogen from wastewater and biowastes can lighten the burden of the environment and save the energy for fertilizer production.

Tyagi and Lo (2013) summarized various conventional and emerging methods for nutrient and energy recycling from sewage sludge as shown in Fig.1-1. In general, bio-chemical and thermo-chemical methods were developed for sewage sludge utilization. Biogas, bio-oil and bio-diesel can be utilized as an energy source. Beyond that, a sequence of sludge derived material can also be recycled such as bio-plastics, metals and fertilizers.

For phosphorus and nitrogen recovery from wastewater and biowastes, various techniques have been attempted. For the solid waste, phosphorus and nitrogen should be released into the liquid phase in the first step. Accordingly, many pretreatment methods have been developed including ultrasonic, incineration, pyrolysis and hydrothermal treatment (Berge et al., 2011; Hossain et al., 2011; Huang & Tang, 2015; Li et al., 2015; Wang et al., 2010).

With regard to ultrasonic pretreatment method, more than 60% of TP was released into liquid after 1 h of sonication. Meanwhile, it also results in 70% of nitrogen released from waste activated sludge. However, a relatively high energy consumption is its main weakness. the sonication intensity needs to be 0.500 W/mL for a good performance on P and N release (Wang et al., 2010).

Except for sonication, a series of thermal treatment method including pyrolysis, incineration and hydrothermal treatment have also been used for sludge treatment. Pyrolysis is a promising method for fertilizer production from biowastes. And how pyrolysis temperature affects P speciation has been widely investigated (Bruun et al., 2017). Research shows that pyrolysis had little effect on P speciation at low temperatures. while apatite was formed as the temperature increased above 600 ºC, which is hard to be absorbed by plants (Bruun et al., 2017). Hydrothermal treatment has also be attempted for sludge treatment (Danso-Boateng et al., 2015; Jain et al., 2016). Compared with other thermal treatment methods, hydrothermal treatment has many advantages such as no pretreatment and easy operation. And valuable products including biochar and hydrolysate containing abundant nutrients were obtained after hydrothermal treatment. Hydrothermal treatment can also be used as a pretreatment method for methane production (Danso-Boateng et al., 2015).

1.2 Hydrothermal technology

1.2.1 Overview

Hydrothermal treatment can be used for converting high moisture content of biosolids at mild reaction temperature into valuable self-separating products, such as biochar with aqueous products and gases (Valdez et al., 2012). It is a promising technology for energy and nutrients recovery from biowastes like sewage sludge without prior drying. During the hydrothermal process, the solid fraction can be separated from the liquid fraction efficiently accompanying by the redistributions of elements. It offers a pretreatment pathway for sewage sludge, which results in not only reducing the volume of sewage sludge but also bringing some byproducts, e.g. biochar and hydrolysate.

Hydrothermal carbonization (HTC), liquefaction and gasification can mainly happen at reaction temperature < 250 ºC, 300 - 350 ºC, and > 350 ºC, respectively (Kumar et al., 2018). Most recently, HTC is paid much attention due to its relatively low operation cost and high resources recovery potential. To date, HTC has been applied for energy and resources recovery from a variety of waste materials such as lignocellulosic biomass (Mäkelä et a;., 2015), Tetra Pak waste (Baskoro, et al., 2017), algae (Lee et al., 2018), and food waste (Zhai et al., 2018).

1.2.2 Fate of phosphorus during HTT

Sewage sludge contains a high amount of phosphorus (P), a valuable resource due to its non-renewable and low reservation nature (US EPA, 1995). As for the fate of phosphorus (P), it has been reported that hydrothermal temperature, feedwater pH and feedstock composition could influence the behavior of P species in sewage sludge (Qian and Jiang, 2014; Wang et al., 2017). Qian and Jiang (2014) claimed that P can be mainly transferred to the fraction easily available to plants in the char at low hydrothermal temperatures (673-873 K), which is replaced by the fraction uneasily absorbed by plants at high temperatures (873-1073 K). In other thermal treatments on sewage sludge like incineration, a similar trend has been observed for P which can be transformed from non-apatite inorganic phosphate (NAIP) to apatite phosphate (AP) in sludge ash at high temperatures (1023-1223 K) (Li et al., 2015). pH also plays an important role in P speciation (chemical state and physical distribution). Wang et al. (2017) claimed that during the hydrothermal processing of sewage sludge at 200-260 °C, the total P (TP) content in biochar can be increased under basic feedwater condition while decreased under an acidic condition in comparison to the neutral condition. P immobilization has also been noticed in the hydrothermal carbonization of manure (Dai et al., 2015). On the other hand, Ekpo et al. (2016) reported that P extraction from manure was pH dependent, and they extracted 94% of P from manure by using 0.1 M H_2SO_4 during HTT. They also claimed that P was mainly retained in the biochar under other tested conditions. Details of P speciation in the biochar have been systematically characterized by Huang and Tang (2016). Their results show that the immobilization of P after the hydrothermal reaction is attributed to the formation of Ca- and Fe-associated P species.

1.2.3 Energy recovery potential of the products

Hydrothermal treatment can also be used for conducting the wet biomass into solid fuel and biocrude. Actually, a series of low-rank materials, including biomass waste and sub-bituminous coal, was subjected to hydrothermal treatment for coalification in the year of 1982 (Ruyter, 1982). In recent years, a wide variety of biowaste, including sewage sludge, alga, food waste, agricultural residues and animal manure were investigated under hydrothermal conditions (Ding et al., 2017; He et al., 2013; Kumar et al., 2011; Oliveira et al., 2013; Toufiq Reza et al., 2016; Valdez et al., 2012). The solid char, which produced

during the hydrothermal treatment is the main energy carrier of the hydrothermal products. Besides, the amount of heavy oil and gases containing H_2 and CH_4 can also be recovered for energy supply source (He et al., 2013).

1.3 Existing problems for current HTT of sewage sludge

Due to the unique advantages regarding the feedstock style and easy operation, HTT is considered as a promising technology for sewage sludge treatment. And many works have been performed on the application of HTT in the past several years. However, HTT still faces many challenges for practical applications.

At first, the diversity of sewage sludge will be a challenge. Sewage sludge produced from different WWTPs in different regions have various performances of HTT depending on the contents of inorganic (e.g. minerals) and organic (e.g. proteins, lipids and carbohydrates) components. For instance, P immobilization and reclamation is a research hotspot. It has been reported that hydrothermal temperature and feedwater pH could influence the behavior of P species in sewage sludge (Inoue et al., 1997; McGaughy and Reza., 2018). Minerals played an important role in P immobilization and reclamation during HTT. Whereas we know little on the effects of the major metal ions on sewage sludge, as well as their competitive relationship during HTT. The binding capacity of different metal ions with P deserved more research for a better utilization of HTT products.

Secondly, as a result of the rapid degradation of the organic component, HTT is considered as an efficient pretreatment method for anaerobic digestion. Energy can be recycled from the methane produced from the anaerobic digestion of high organic HTT liquid. However, a large amount of P will still exist in the liquid fraction, which resulted in the wasting of resources. Most previous studies forced on the reclamation of P in the solids. P in HTT liquid products should be appreciated and a proper recovery method for P recovery from the high organic liquid should be developed.

At last, HTT is an energy consumption process. The process energy balance significantly influences the energy costs. Therefore, how to increase the overall energy efficiency is crucial for the economic aspect of HTT. Two important aspects must be considered to improve the energy efficiency of HTT. Firstly, it is important to reduce the amount of water in the feedstock. The latent heat of vaporizing 1 kg of water was 3.15 MJ, resulting in a substantial energy consumption during the sludge drying process (Wang et al., 2018). And the sewage sludge with a higher dry matter content could produce more

hydrochars. Next, a proper HTT temperature is a critical factor for energy saving. The excess temperature may result in the decreased in the yield of hydrochar which further reduced the energy output. Therefore, HTT temperature should be optimized carefully in the energy aspect.

1.4 Objectives and thesis structure

In this study, HTT of sewage sludge was investigated to explore the options for nutrients and energy recovery from the sludge. The major purpose of this work was to fully evaluate the nutrients and energy recovery potentials from the sewage sludge, including primary sludge, digested sludge and AGS from UASB reactor. The main objectives of this research are as follows:

a) The effects of minerals additives on P mobility and immobilization during HTT were evaluated;
b) Different HTT conditions including temperature and reaction time were evaluated to maximize P recycle.
c) The key parameters of the crystallization process including pH and Mg/P molar ratio were optimized to recycle the struvite precipitate;
d) Mass balance in the HTC products and the energy balance during the HTC process were analyzed.
e) The properties of produced hydrochar including HHVs, combustion behavior and elemental composition were evaluated for further application.

1.5 Structure of this research

The main content of this thesis is composed of three parts. One aspect of this study was focused on nutrients (mainly P) recovery from the sewage sludge by investigating the relationship between P and minerals in the primary sludge during HTT in Chapter 2 and the development of P recovery method by using struvite precipitation in Chapter 3. Another aspect of this study focused on evaluating energy recovery potentials from hydrothermal products of AGS in Chapter 4.

The thesis structure is displayed in Figure 1-1.

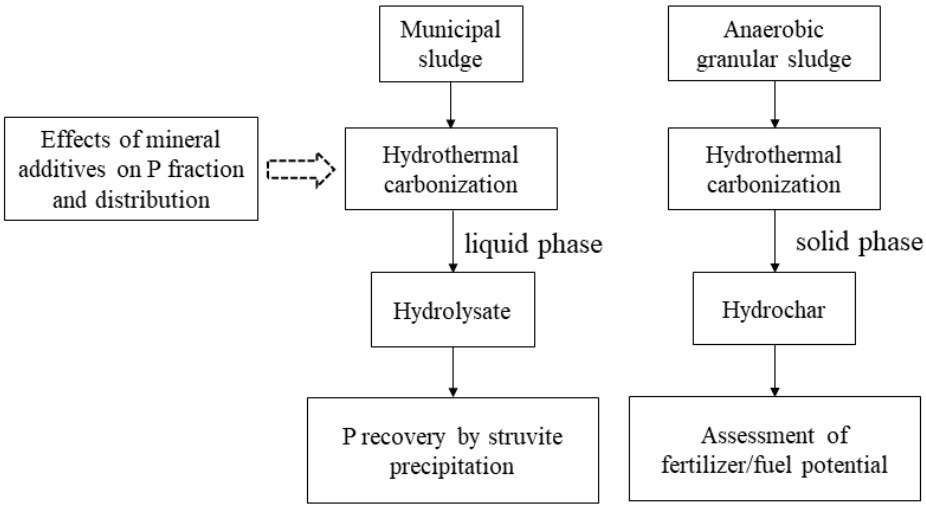

Figure 1-1. Experimental structure of this study.

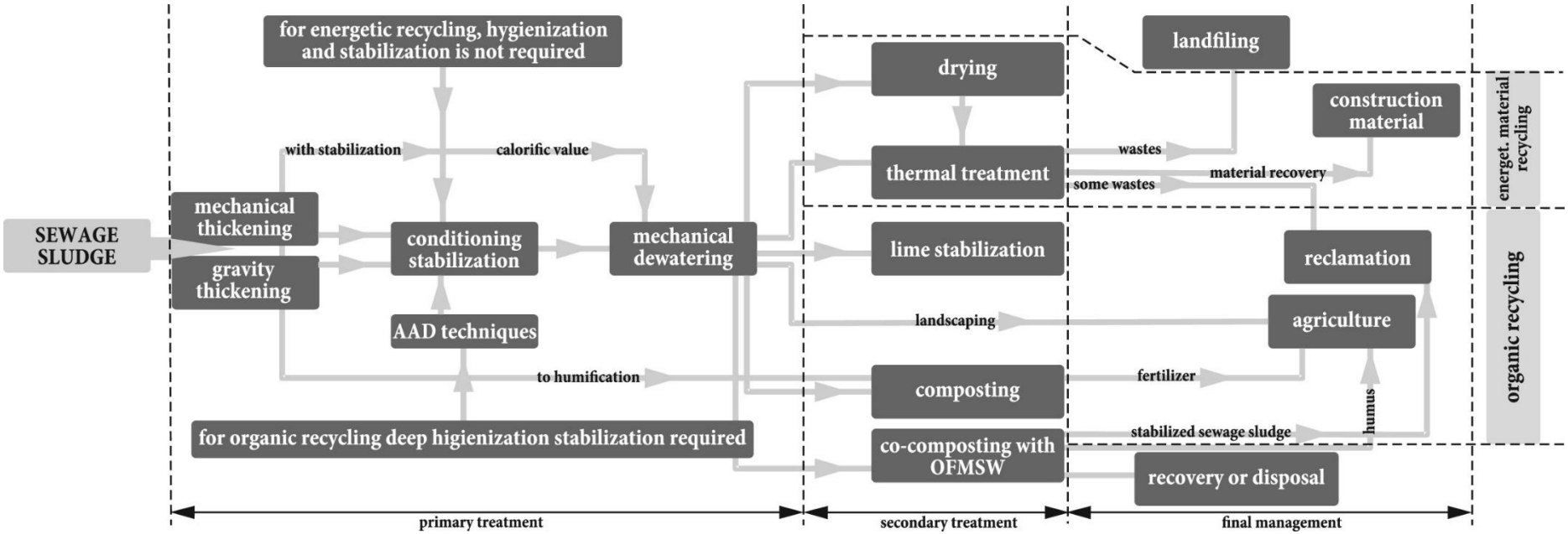

Fig. 1- 2 The typical treatment process for sewage sludge produced from WWTPs (Kacprzak et al., 2017)

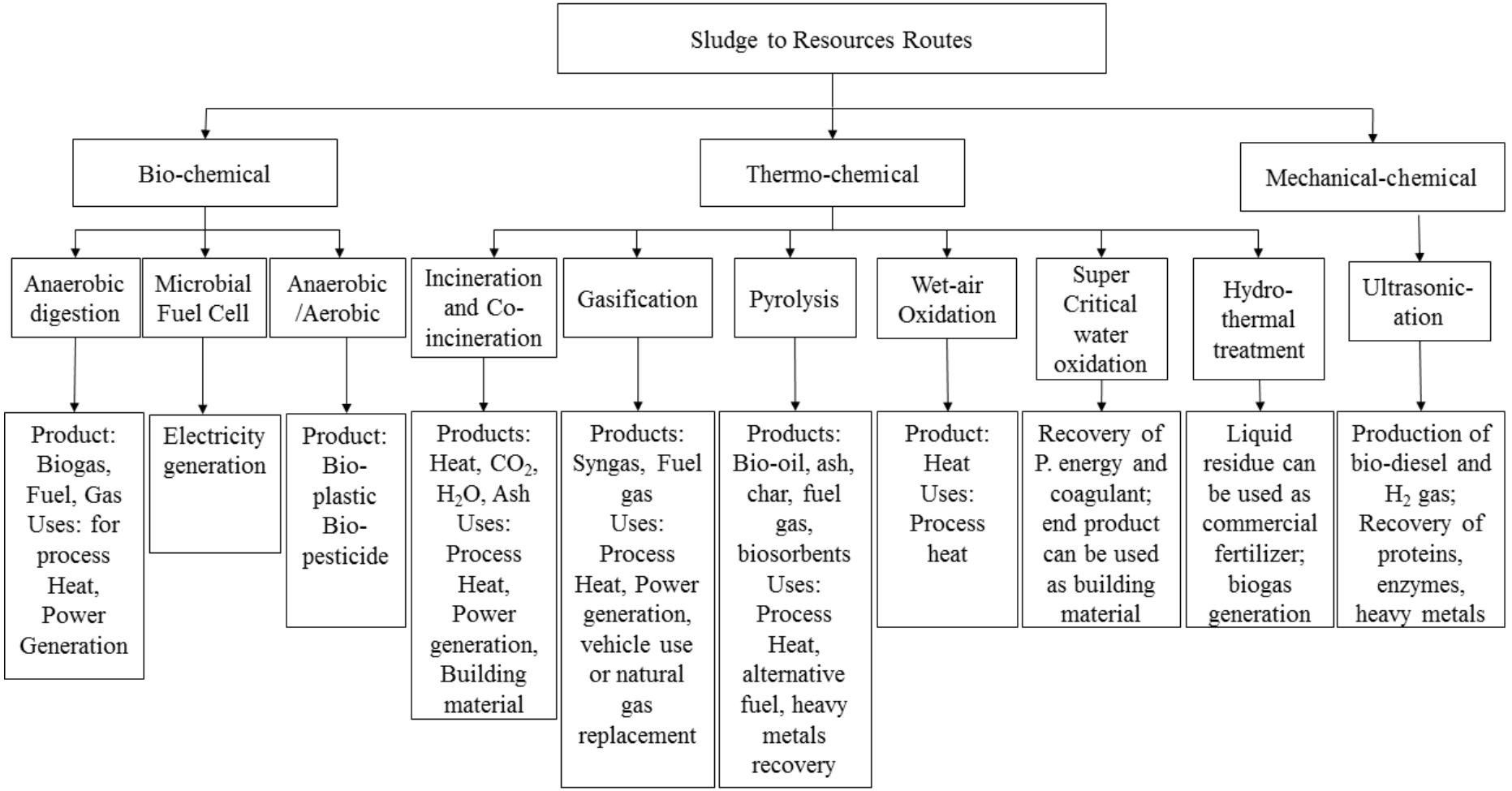

Fig. 1- 3 Various methods for resource recovery from waste sludge (Tyagi & Lo, 2013)

Chapter 2 Effects of mineral additives on P immobilization from sewage sludge using hydrothermal treatment

2.1 Introduction

In view of the critical role for P immobilization, the effects of major minerals such as Ca, Fe and Al in sewage sludge, as well as their competitive relationship during hydrothermal treatment deserve more detailed investigation. Still, very limited information is available regarding this aspect. This study aims to evaluate the priority order among the three minerals in the sludge when reacting with P during HTT. Besides, the binding capacity of each mineral was assessed by adjusting their content in the sludge. The characterization of the biochar produced was also performed. This work is expected to provide basic knowledge of the relationship between P speciation and minerals during HTT, which is the key to P immobilization and recycling from biomass.

2.2 Materials and methods

2.2.1. Materials

Concentrated primary sludge used in this study was sampled from a wastewater treatment plant in Ibaraki Prefecture, Japan. The sludge was kept at 4 °C in the refrigerator prior to use. The sludge was manually stirred completely before being used for HTT. Table 2-1 shows the main physicochemical characteristics of the raw sludge.

2.2.2 Hydrothermal treatment procedure

The hydrothermal experiments were performed in a 200 mL stainless-steel cylindrical reactor (MMJ-200, OM Labtech Co., Japan). A series of runs were performed with different kinds and amounts of minerals to investigate the effects of P immobilization and biochar production. Fe, Ca and Al have been reported to have predominant effects on P immobilization in the sludge, which may also have obvious impacts on P speciation (Caravelli et al., 2010; Carlsson et al., 1997; Yang et al., 2006).

Before HTT, 5 or 10 mmol of single mineral ($FeCl_3$, $CaCl_2$ or $AlCl_3$) or equal molar mixture (5/3 mmol or 10/3 mmol of $FeCl_3$, $CaCl_2$ and $AlCl_3$) was individually added into 180 mL of sludge. The test conditions were labeled as Fe (Ca or Al)-5 or Fe (Ca or Al)-10, and Mix-5 or Mix-10 when 5 mmol of Fe (Ca or Al) or 10 mmol of Fe (Ca or Al), and the mixture additives were added, respectively. After mineral(s) addition, the sludge sample was stirred by a magnetic stirrer at 100 rpm for 10 min. Then the sludge was loaded into the hydrothermal reactor. No additional pH adjustment was conducted during the treatment. The HTT temperature was determined at 200 °C according to a previous research with a holding time of 60 min. The hydrolysate and biochar were separated by centrifugation at 9000 rpm for 10 min followed by vacuum filtration using 25 μm filter paper. The hydrolysate was preserved in the refrigerator at 4 °C before being analyzed. The obtained biochar was dried at 60 °C for 2 days, then ground into fine powders and stored in enclosed plastic bags until analysis.

2.2.3. Analytical methods

Soluble P was measured in accordance with the standard methods using a UV-Vis spectrophotometer (Shimadzu UV-1800, Japan) (APHA,1998). Soluble total organic carbon (TOC) was analyzed by a TOC analyzer (Shimadzu TOC-V_{CSN}, Japan) after filtration through a 0.22 μm membrane (PTFE, Membrane Solutions, US). pH was determined with a pH meter (Mettler Toledo FE20, Switzerland). The metal ions in the hydrolysate were quantified using ICPS (Shimadzu ICPS-8100, Japan) after being completely digested with nitric acid and hydrogen peroxide at 98 °C.

For the solid samples, the amount of P in each sample was analyzed using the SMT procedure (Ruban et al.,1999). P in solids can be divided into inorganic P (IP) and organic P (OP). IP can be further classified into two categories: NaOH-P (non-apatite IP, or NAIP) and HCl-P (apatite phosphate, or AP). NAIP is mainly composed of the fraction associated with Al, Fe and Mn oxides and hydroxides, which together with OP is usually supposed to be active and can be utilized by plants. Ca-P compounds are referred as AP which usually remains stable and might cause less P loss-related problems (Huang and Tang, 2016).

The contents of C, H and N in the sludge and the hydrothermal residue were determined by an elemental analyzer (PerkinElmer 2004 CHN, USA). Thermal analysis of the biochar was performed by a thermal analyzer (Seiko TG/DTA7300, Japan) with

the temperature increased from 323 K to 873 K at a heating rate of 10 K min^{-1} in an air atmosphere. The biochar was also characterized by Fourier Transform Infrared (FTIR) spectroscopy (JASCO FT/IR -300, Japan) at the range of 4000-400 cm^{-1}. The X-ray powder diffraction (XRD; Bruker D8 FOCUS, USA.) data were collected with Cu/K radiation source (40kV 40mA) over a range of 10-70º 2θ-angle in 0.02 step sizes with an integration time of 0.6 s.

2.2.4. Statistical analysis

All the results are expressed as the mean values of triplicate tests. The experimental data were analyzed using the software IBM SPSS 24.0 (SPSS, Inc., USA) for Windows. Pearson correlation was used to evaluate the relationship between the P speciation and mineral additives during HTT.

2.3 Results and discussion

2.3.1 Mineral addition on phosphorus immobilization in sludge during HTT

The sludge was first hydrothermally treated together with 5 or 10 mmol of Fe, Ca, Al or their mixtures. Fig. 2-1 shows the TP and total ammonium nitrogen (TAN) concentrations in the hydrolysate after HTT at 200 ºC for 1 h. TP concentration in the hydrolysate without mineral addition is 703.09 mg/L, accounting for 60.0% of TP in the sludge. The high ionic strength (Fe^{3+}, Ca^{2+} or Al^{3+}) in sludge significantly affects the existing form of P in hydrolysate (Fig.2-1): The TP concentration decreased to 344.63 mg/L and 262.70 mg/L after 5 and 10 mmol of Fe^{3+} addition, respectively. A close relationship between Fe and P has been observed in sludge by Wilfert et al. (2015) and Wu et al. (2015). As seen, some of P in sludge exists in the form of distinct Fe-PO_4 minerals while some as P adsorbed onto iron oxyhydroxide minerals (Wu et al., 2015). Huang and Tang (2016) pointed out that Fe-associated P increased after HTT for 4 h, from 2.3% in the raw activated sludge to 13% in its hydrochar. Table 2-2 shows that the concentration of ferric ions decreased from 1572.72 (Fe-5) and 3123.97 mg/L (Fe-10) to 200.12 and 1202.61 mg/L, respectively. After HTT, however, Ca concentration increased with the addition of Fe additive, indicating that Fe is more competitive than Ca for bonding with P during the hydrothermal process.

Equimolar Ca ions addition showed better performance than Fe in P immobilization during HTT. The TP concentration decreased to 211.49 and 116.76 mg/L when 5 and 10 mmol Ca^{2+} were added, respectively (Fig. 2-1). Unlike Fe, Ca usually combines with P directly to form calcium phosphate precipitates. The relationship among the decrease in P solubility, the increased AP, and the decreased soluble Ca after HTT has been observed during the hydrothermal carbonization of cow manure (Dai et al., 2015). As displayed in Table 2-2, the concentration of Ca decreased after the hydrothermal reaction, from 1224.70 (Ca-5) and 2337.98 mg/L (Ca-10) to 30.43 and 437.53 mg/L, respectively, signaling the formation of Ca-P precipitates.

Among the tested three minerals, Al showed the best performance for P immobilization. TP concentration decreased to 83.47 and 42.50 mg/L when 5 and 10 mmol of Al^{3+} were applied, respectively, meaning that 92.89% and 96.38% of P was immobilized in the produced biochar. Compared with Fe, Al-phosphate has a lower solubility. Therefore, P can bind with Al to form more stable and stronger compounds. As shown in Table 2-2, only Al ions decreased dramatically, while both Ca and Fe concentrations increased greatly after 10 mmol of Al additive was applied. This observation indicates that P prefers to combine with Al instead of Ca and Fe during HTT.

When the HTT was performed after addition of the equimolar mineral mixtures, i.e. the last two conditions (Mix-5 and Mix-10), results revealed that Al^{3+} is still the most competitive one to bond with P during HTT. With a total molar amount of 10 mmol, the Al, Fe and Ca concentrations decreased by 3.32 mmol, 1.26 mmol and 0.66 mmol, respectively.

2.3.2 Mineral addition on phosphorus fractionation in the produced biochar

Figure 2-2 shows the change of P fractions in the biochar produced from HTT of primary sludge by using the SMT protocol. The SMT protocol can be used to not only identify the P bonded with different kinds of minerals but also evaluate the bioavailability potential and mobility of P in the produced biochar. The results show that IP was the predominant fraction of TP in the biochar without mineral addition (control), about 99.6% (Figs. 2a and 2b), in which NAIP and AP fractions account for 54.6% and 44.9%, respectively.

The TP content in the biochar increased obviously, from 12.59 mg/g to 16.91 and 30.45 mg/g when 5 and 10 mmol Fe^{3+} were applied, respectively. Correspondingly, the NAIP content increased from 6.88 mg/g to 16.61 and 29.25 mg/g, respectively. However, the AP content decreased from 5.66 mg/g in the biochar without mineral addition (control) to 3.01 (Fe-5) and 0.14 mg/g (Fe-10), respectively. This remarkable decrease indicates that even though Ca binds with P strongly, Fe can compete against Ca to combine with P under the tested HTT conditions (Figs. 2-2 c and d).

As for Ca addition, the TP content in biochar increased to 27.53 and 31.74 mg/g when 5 and 10 mmol Ca were applied for HTT of sludge. The TP content in biochar at 5 mmol Ca application is higher than that at 5 mmol Fe application, implying equimolar amounts of Ca can immobilize more P in biochar during HTT. As P can mainly combine with Ca in the form of AP, it's understandable that the AP content in biochar increased, which amounted to 82.6% and 85.9% of the TP in biochar when 5 and 10 mmol Ca were applied, respectively (Figs. 2-2 e and f).

When 5 and 10 mmol Al were applied in the HTT process, the P content in biochar was 33.68 mg/g and 43.89 mg/g, in which NAIP content was 32.63 mg/g and 43.70 mg/g, respectively. Clearly and interestingly, almost no AP was detected in the produced biochar under the addition of Al^{3+} conditions (Figs. 2-2 g and h). This observation implies that if there is enough Al existing in the sludge, P tends to combine with Al rather than Ca and Fe during the HTT process.

On the other hand, the competitiveness among the three mineral additives for P immobilization are also explored in this work. When equimolar amounts (5/3 or 10/3 mmol) of Fe, Ca and Al (at the total mineral addition of 5 or 10 mmol) were applied to HTT of sludge, the TP and AP contents in biochar were 26.98 and 12.94 mg/g, respectively. When a total of 10 mmol of these three minerals were applied, the TP content in biochar increased to 33.10 mg/g, while the AP content remained almost unchanged, about 12.37 mg/g. This observation indicates that the increase of TP content in the biochar is mainly determined by NAIP. By measuring metal contents in the produced biochar, compared to the biochar from Mix-5 addition, Ca content decreased from 16.02 mg/g to 7.30 mg/g in the biochar after Mix-10 addition, while Fe and Al contents increased from 16.35 and 10.42 mg/g to 18.85 and 18.76 mg/g, respectively. This result confirms that with enough metal ions co-existing in the sludge, P is most inclined to combine with Al and then followed by Fe during HTT.

The results from Pearson correlation analysis between different minerals and P fractionation are presented in Table 2-3. According to Table 2-3, Fe has no significant Pearson correlation with all P fractions during HTT of sludge. A variety of reasons can be attributable to the P-Fe interaction which can be either iron phosphate minerals or adsorption complexes (Frossard et al., 1997; Smith et al., 2008). A strongly positive correlation was found between the initial Ca content and AP content ($R = 0.937$; $p < 0.01$). This result suggests that the AP amount in biochars produced from HTT of sludge has a linear relationship with the initial Ca concentration in the sludge. More importantly, Al shows a positive correlation with NAIP ($R = 0.811$; $p < 0.05$). These results indicate that it is feasible to recover P from sewage sludge as a more bioavailable form by adding Al^{3+} during HTT.

2.3.3 Biochar characterization

The FTIR spectra analysis of the biochar samples is conducted. As shown in Fig. 2-5, the broad and strong band at near 3400 cm^{-1} can be attributed to OH groups in all samples (Stevenson and Goh, 1971). Two strong adsorptions at 2920 and 2850 cm^{-1} are assigned to aliphatics. The 1710 cm^{-1} band is attributed to fulvic acid, indicating that the produced biochar is a potential material to improve soil quality. The bands near 1540 and 1640 cm^{-1} are assigned to peptide (Stevenson and Goh, 1971). In addition, all the biochars exhibit strong vibrational bands between 900 and 1300 cm^{-1} relating to PO_4 (Franca et al., 2014). As for the biochar from Ca-10 addition, the bands at 550-700 cm^{-1} might be from the overlap of PO_4 and OH libration modes (Franca et al, 2014).

The crystalline properties of the biochar samples were characterized by using XRD. From the XRD patterns (Fig. 2-6), the minerals presented in the biochar is consistent with the above observations. As for the HTT with Fe addition (Fe-10), iron hydrogen phosphate, iron phosphate hydroxide and iron hydrogen phosphate were found as the main components in the produced biochar. As for Ca-10, calcium phosphide, hydroxylapatite and calcium phosphate were determined as the main phosphate minerals. In the case of Al-10, a variety of Al-P minerals (aluminum phosphate, sodalite, aluminum phosphate and aluminum phosphide) were formed. At last, as per the Mix-10, P was found to mainly bind with the three minerals. Namely, aluminum phosphate, iron phosphate and calcium hydrogen phosphate are co-existing in the produced biochar (Mix-10).

2.3.4. Other additional information about the hydrolysate produced in this work

Mineral additive addition led to an increase in TAN as shown in Fig. 2-1. This observation might be brought about by accelerated deamination reaction due to the addition of these additives. He et al. (2015) pointed out that the addition of CaO can accelerate the deamination of stable organic-N to ammonium. Results from this work demonstrated that other minerals like Fe and Al can also accelerate the deamination reaction. Among the tested three minerals, Al showed the best catalytic effect, resulting in TAN concentration increased from 558.39 mg/L to 798.86 mg/L after HTT at 200 ºC for 1 h with 10 mmol of Al^{3+} addition.

The soluble TOC and pH of the hydrolysate are shown in Fig. 2-3. Mineral additive addition can decrease sludge pH to some extent. $FeCl_3$ addition at 5 and 10 mmol caused the largest drop in sludge pH from 6.83 to 4.37 and 3.26, respectively. Ca and Al minerals show a similar performance, and the hydrolysis of minerals brings about the decreased pH to some extent. HTT further promotes the pH decrease, which is usually explained by the evolution of organic substances (Wang and Li, 2015). Obviously, the effect of hydrolysis has been ignored. In this study, the VFAs production shows no significant difference among the different mineral additive conditions (Fig. 2-4), indicating that the VFAs production is not the only reason bringing about the decrease in sludge pH. In addition, compared to Ca addition, an equal mole of Fe or Al addition resulted in lower pH, i.e. about 2.53 or 2.25 at 10 mmol of addition, respectively. This phenomenon can be interpreted as Ca is existing as a divalent cation and Fe and Al are trivalent cations. Equal molar amount of Fe and Al can release more hydroxyl than Ca during the hydrolysis process. Above all, Al plays the largest role in influencing pH during HTT. The soluble TOC was found to have a negative correlation with hydrolysate pH. The highest level of soluble TOC (7991.2 mg/L) was achieved at pH 2.25 after addition of 10 mmol Al additive. These results show that low pH is beneficial for dissolution of organic substances during HTT.

2.4 Summary

HTT as an emerging method has been applied for efficient treatment of biomass wastes. This part explored the effects of mineral additives on phosphorus(P) immobilization and biochar production from primary sludge by using HTT. Different

minerals including ferric(Fe), calcium(Ca) and aluminum(Al) were added into the sludge to probe P immobilization and mechanisms involved during HTT. All the three minerals demonstrated significant effects on P immobilization, among which Al was the most efficient effector, yielding 92.89% and 96.38% of P immobilization respectively at 5 and 10 mmol of Al mineral additives. Both Al and Fe rather than Ca promoted the formation of non-apatite inorganic phosphate (NAIP) and reduced the amount of apatite phosphate (AP) in the biochar. Moreover, results from this study indicate that during HTT, Al-P is the primary existing form in the biochar when phosphate reacts with the tested three metals co-existing at equimolar quantity in the sludge.

Tables

Table 2-1 Main physicochemical characteristics of the raw primary sludge used in the experiments.

Parameters	Sewage sludge	Unit
Total solids (TS)	3.35	%
Volatile solids (VS)	76.61	% of TS
Carbon	46.32	% (dw)
Nitrogen	5.25	% (dw)
Phosphorus	3.50	% (dw)
pH	5.03	

dw, dry weight of the sludge

Table 2-2 Minerals concentration in the hydrolysate obtained from HTT of sludge after addition of different mineral additives.

	Initial concentration (mg/L)			Final concentration (mg/L)			Total reduction （mmol）		
Mineral(s)	Fe	Ca	Al	Fe	Ca	Al	Fe	Ca	Al
Initial	21.47	111.42	1.41	6.35	79.68	0.42	0.05	0.14	0.01
Fe-5	1572.72	111.42	1.41	200.12	146.77	1.51	4.42	-0.16	0.00
Fe-10	3123.97	111.42	1.41	1202.61	457.02	4.09	6.19	-1.55	-0.02
Ca-5	21.47	1224.70	1.41	1.30	30.43	1.42	0.36	5.36	0.00
Ca-10	21.47	2337.98	1.41	8.66	437.53	3.05	0.23	8.53	-0.01
Al-5	21.47	111.42	750.85	18.36	207.10	1.99	0.06	-2.39	5.00
Al-10	21.47	111.42	1500.29	132.30	480.96	208.42	-1.98	-1.66	8.62
Mix-5	538.55	482.51	251.22	101.22	165.76	0.63	1.41	1.42	1.67
Mix-10	1055.63	853.61	501.04	657.81	706.16	2.52	1.26	0.66	3.32

Note: -5 or -10 denotes that 5 or 10 mmol of the designated mineral(s) was added into the sludge before HTT.

All data are the average values of triplicate tests.

Table 2-3 Pearson correlation coefficients between various minerals and P fractionation.

		TP	IP	AP	NAIP
Initial Fe	Pearson Correlation	-0.350	-0.341	-0.436	0.147
	Sig. (2-tailed)	0.395	0.409	0.280	0.729
	Sum of Squares and Cross-products	-368.460	-359.082	-652.894	293.812
	Covariance	-52.637	-51.297	-93.271	41.973
	N	8	8	8	8
Initial Ca	Pearson Correlation	-0.002	-0.086	0.937**	-0.745*
	Sig. (2-tailed)	0.997	0.839	0.001	0.034
	Sum of Squares and Cross-products	-1.676	-91.139	1402.254	-1493.392
	Covariance	-0.239	-13.020	200.322	-213.342
	N	8	8	8	8
Initial Al	Pearson Correlation	0.802*	0.845**	-0.491	0.811*
	Sig. (2-tailed)	0.017	0.008	0.217	0.015
	Sum of Squares and Cross-products	843.590	890.766	-734.425	1625.191
	Covariance	120.513	127.252	-104.918	232.170
	N	8	8	8	8

* Correlation is significant at the 0.05 level (2-tailed).

** Correlation is significant at the 0.01 level (2-tailed).

TP indicates total phosphorus; IP indicates inorganic phosphorus; AP indicates apatite phosphorus; NAIP indicates non-apatite inorganic phosphorus

Table 2-4 The mass balance of P in solid and hydrolysate after HTT.

Samples	P in solid		P in hydrolysate	
	mg	%	mg	%
Control	83.99	40.13	126.56	60.47
Fe-5	143.54	69.82	62.03	30.18
Fe-10	167.19	77.95	47.29	22.05
Ca-5	174.00	82.05	38.07	17.95
Ca-10	186.65	89.88	21.02	10.12
Al-5	199.70	93.00	15.02	7.00
Al-10	205.39	96.41	7.65	3.59
Mix-5	159.21	75.42	51.89	24.58
Mix-10	179.74	87.13	26.55	12.87

Control means the hydrothermal treated sludge without any mineral additives. -5 or -10 denotes that 5 or 10 mmol of the designated mineral(s) was added into the sludge before HTT.

Figures

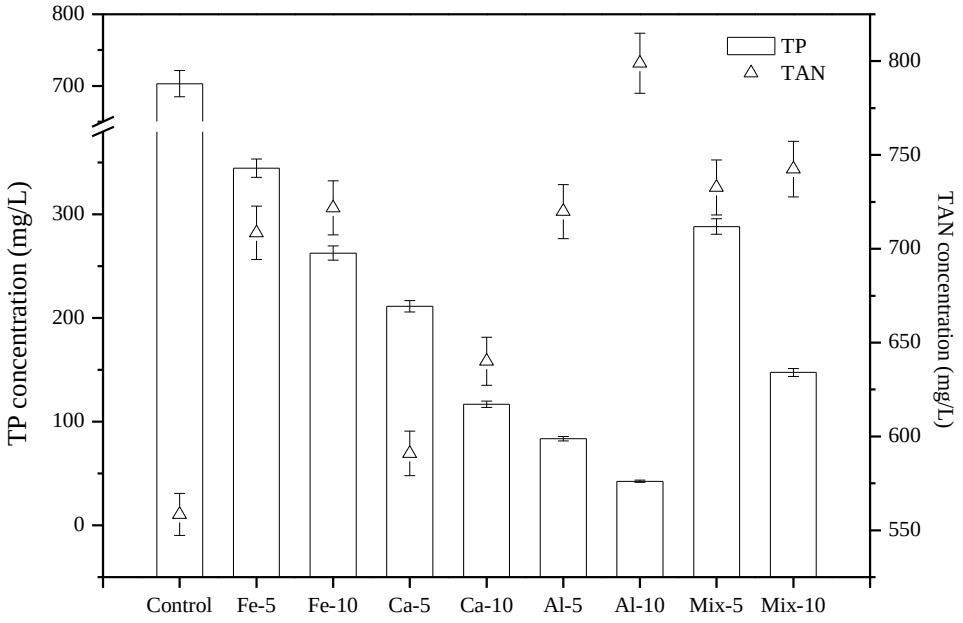

Fig. 2-1 Effects of different mineral additives on TP and TAN concentrations in the hydrolysate.

TAN-total ammonia nitrogen, TP-total phosphorus. Control means the hydrothermal treated sludge without any mineral additives. -5 or -10 denotes that 5 or 10 mmol of the designated mineral(s) was added into the sludge before HTT.

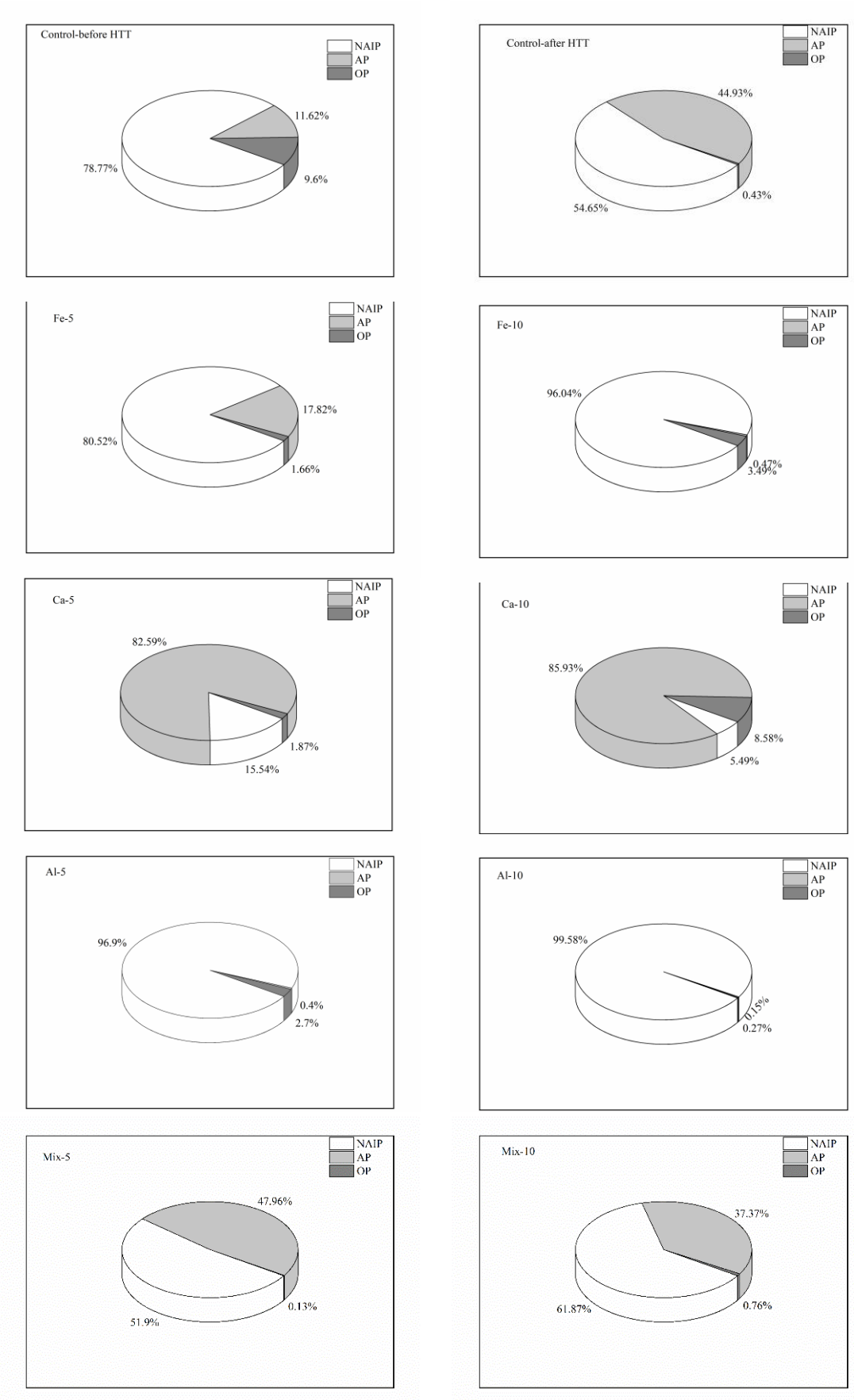

Fig. 2-2 Effects of different mineral additives on P speciation in sludge after HTT.

Control means the hydrothermal treated sludge without any mineral additives. -5 or -10 denotes that 5 or 10 mmol of the designated mineral(s) was added into the sludge before HTT.

IP indicates inorganic phosphorus; AP indicates apatite phosphorus; NAIP indicates non-apatite inorganic phosphorus

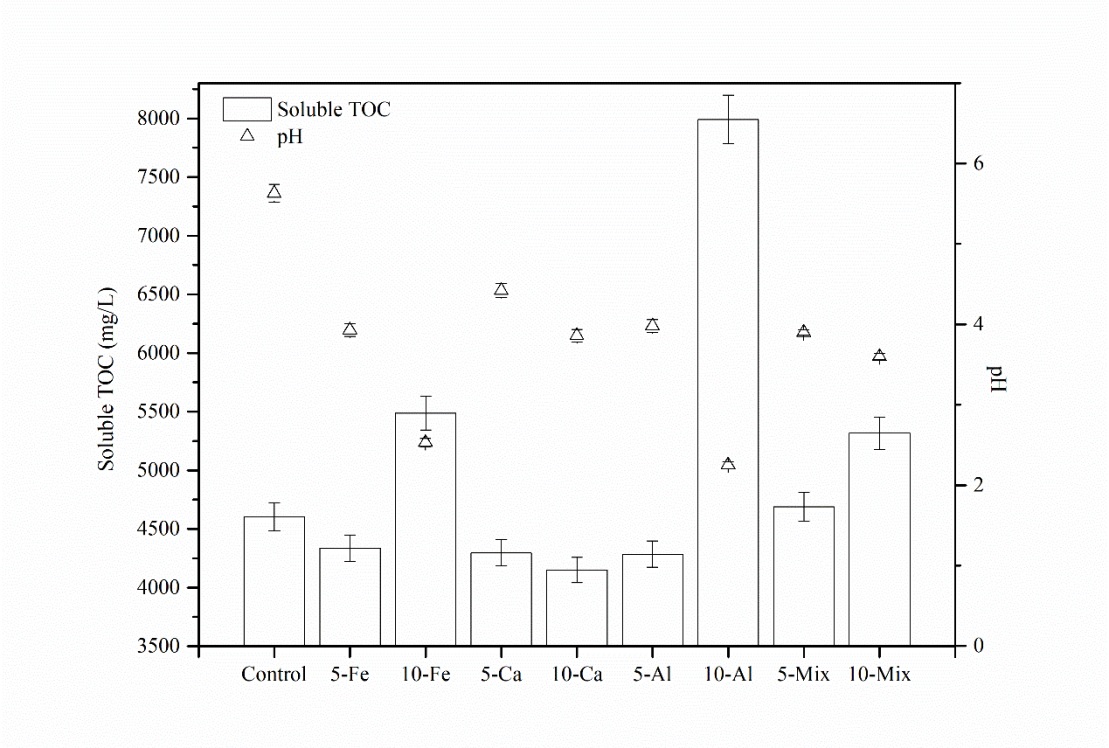

Fig. 2-2 Effects of different mineral additives on soluble TOC concentration and pH in the hydrolysate from sewage sludge.

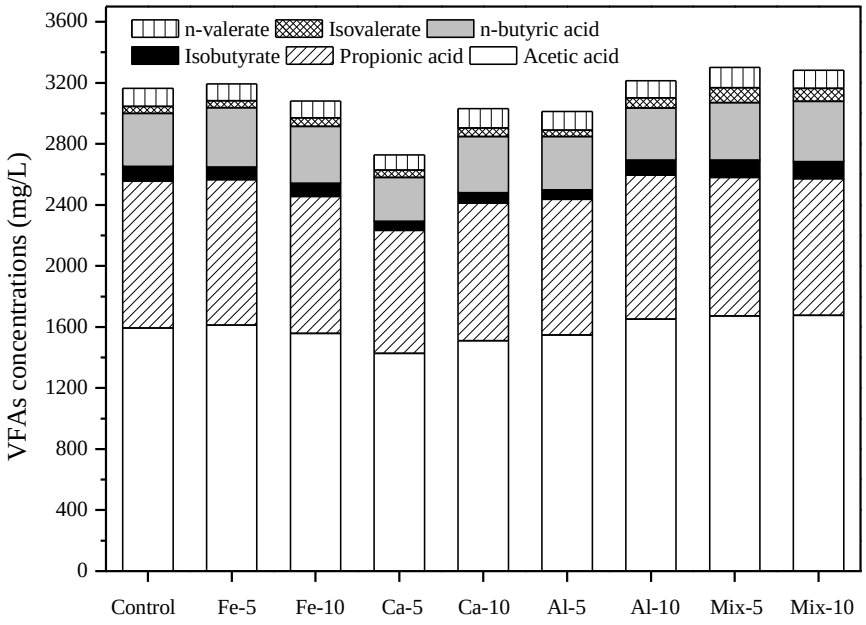

Fig. 2-3 Effects of different mineral additives on VFA production from sludge after HTT at 200 ºC for 1 h.

Control means the hydrothermal treated sludge without any mineral additives. -5 or -10 denotes that 5 or 10 mmol of the designated mineral(s) was added into the sludge before HTT.

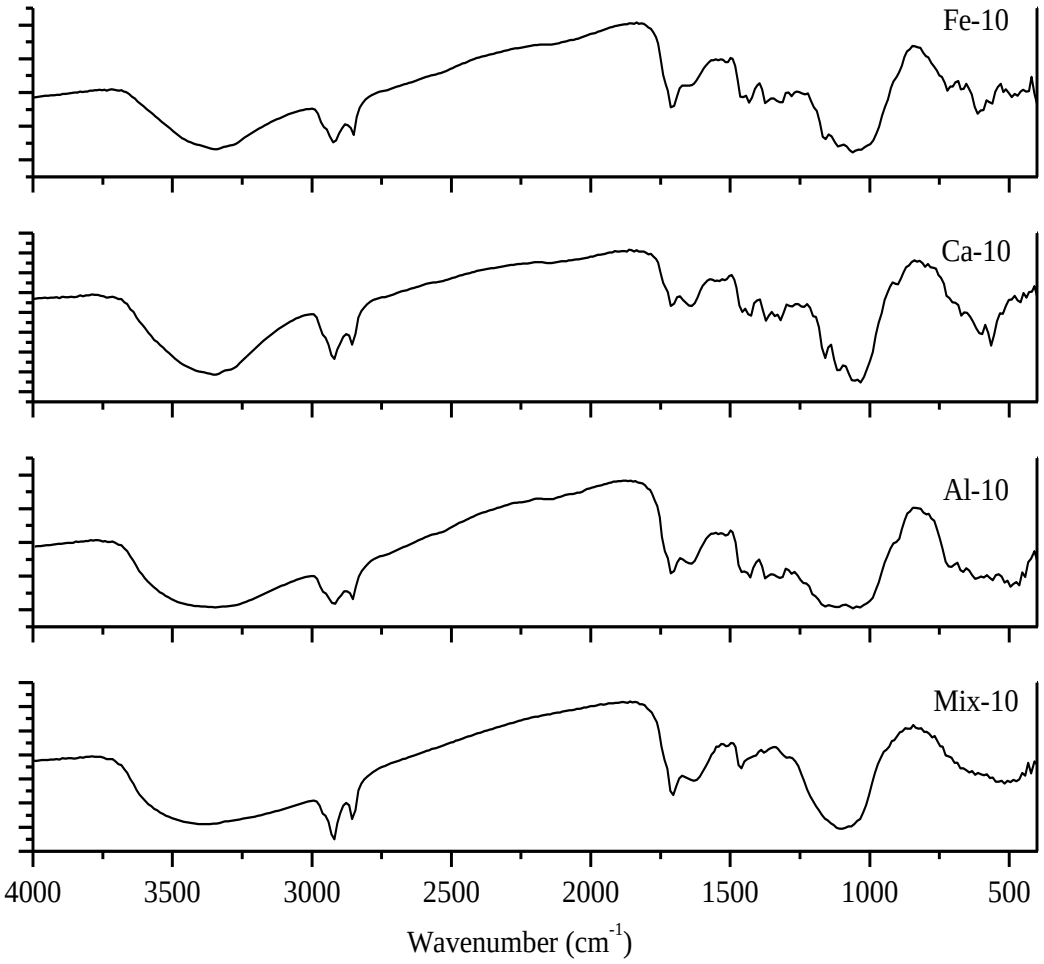

Fig. 2-4 FTIR spectra of Fe-10, Ca-10, Al-10 and Mix-10

-10 denotes that 10 mmol of the designated mineral(s) was added into the sludge before HTC. Initial pH or final pH indicates that the pH measured after minerals added into sludge or after HTC.

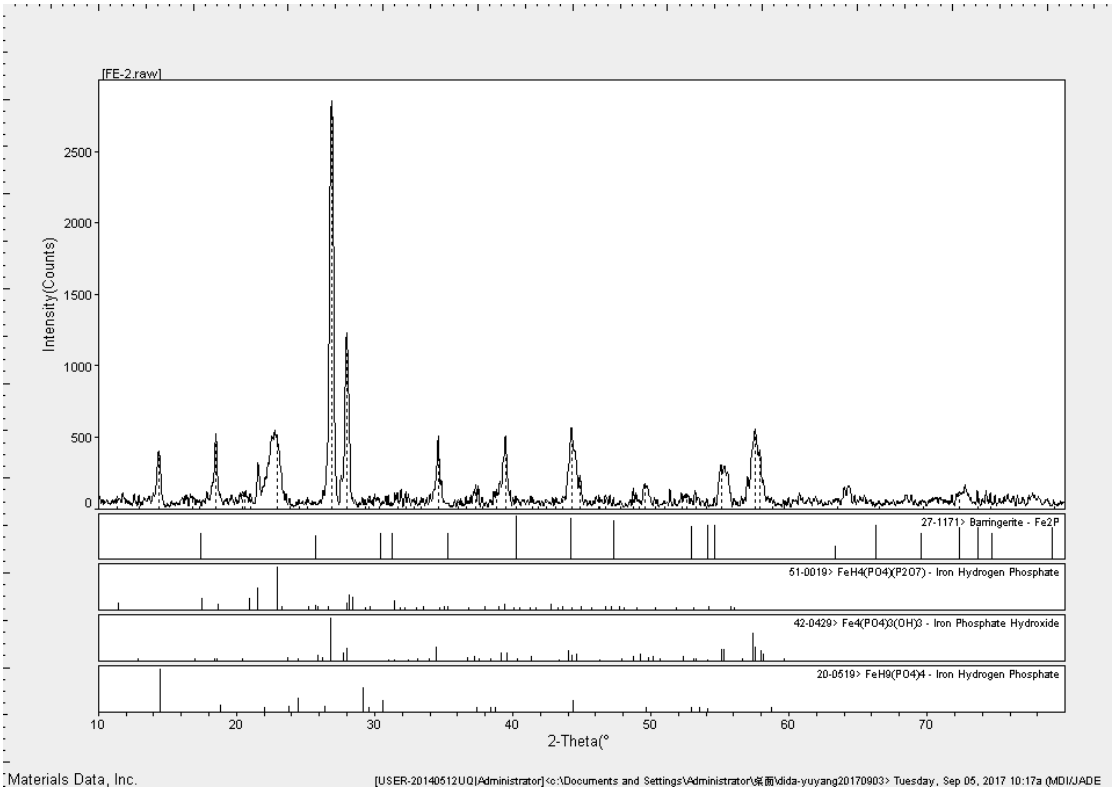

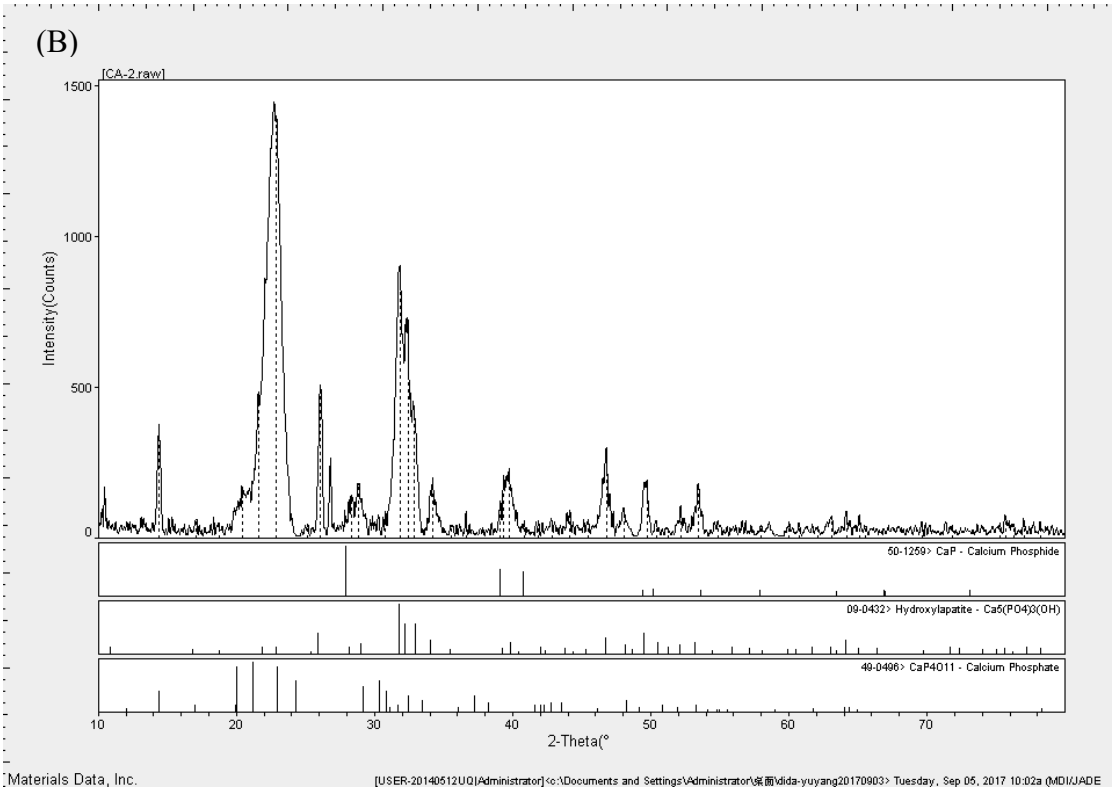

Fig. 2-6a XRD patterns of Fe-10 (A) and Ca-10 (B)

-5 or -10 denotes that 5 or 10 mmol of the designated mineral(s) was added into the sludge before HTC. Initial pH or final pH indicates that the pH measured after minerals added into sludge or after HTC.

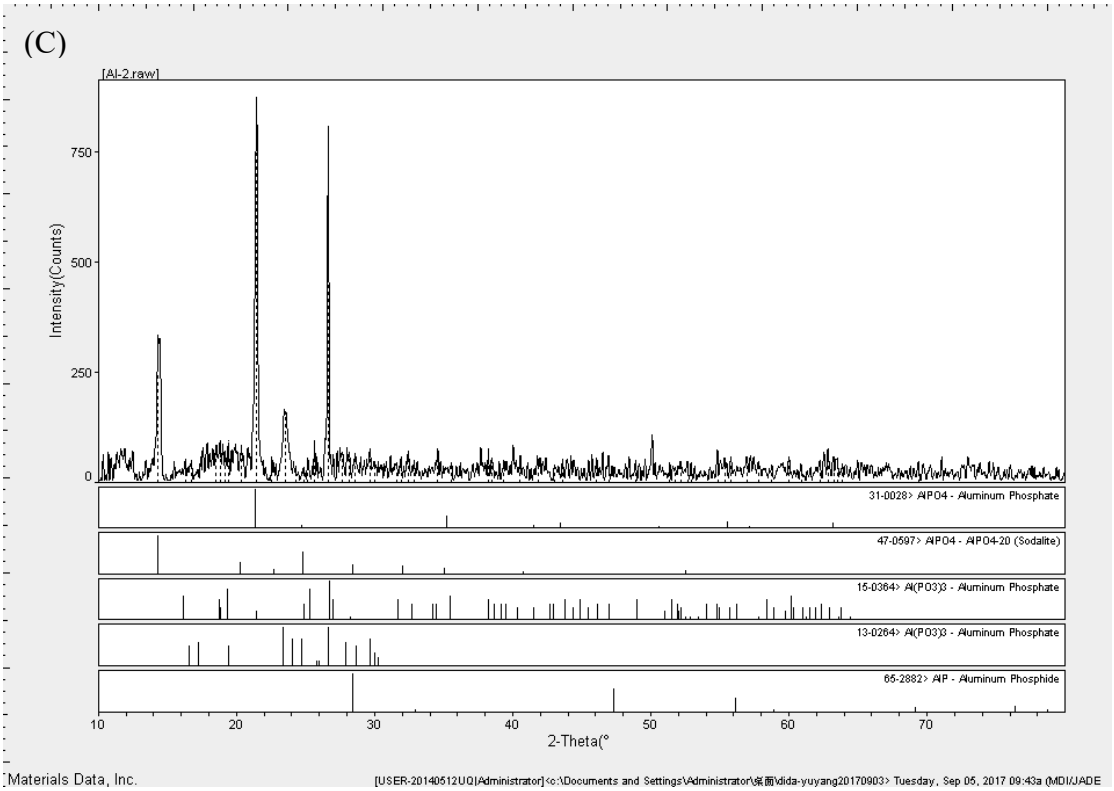

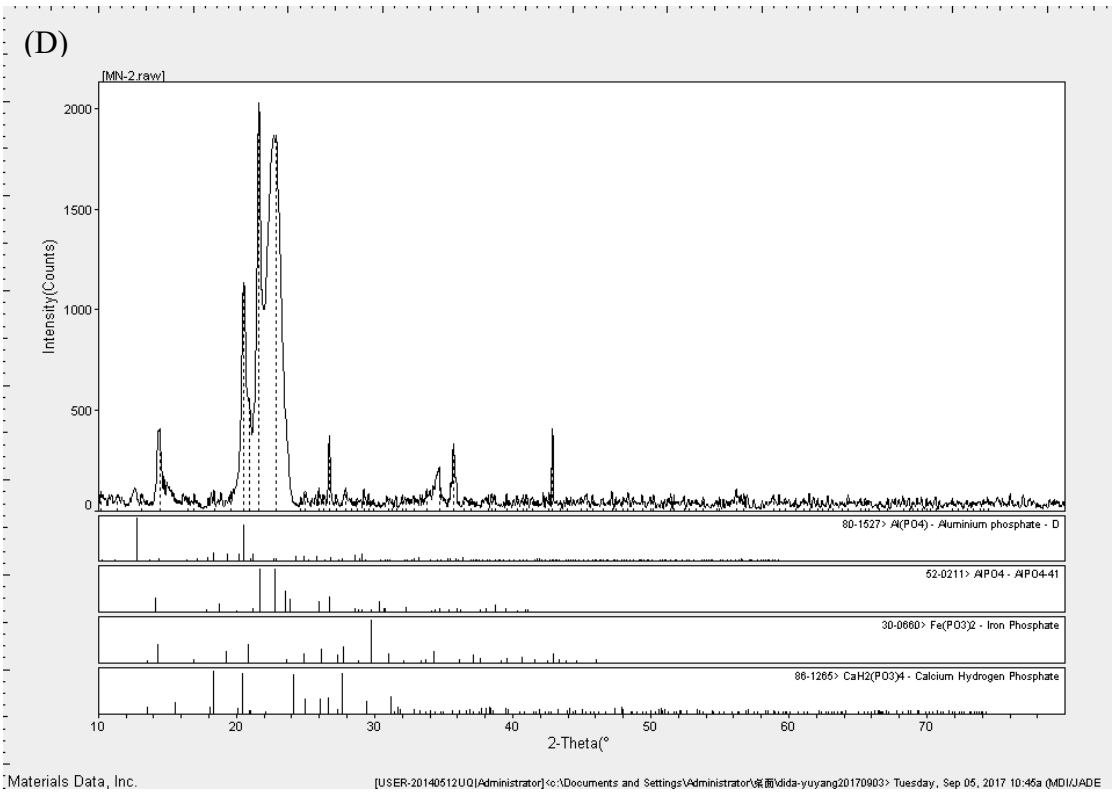

Fig. 2-6b XRD patterns of Al-10 (C) and Mix-10 (D)

-5 or -10 denotes that 5 or 10 mmol of the designated mineral(s) was added into the sludge before HTC. Initial pH or final pH indicates that the pH measured after minerals added into sludge or after HTC.

Chapter 3 P and N recovery from sewage sludge using a hybrid system coupling hydrothermal pretreatment with struvite precipitation

3.1 Introduction

Hydrothermal treatment is proposed to release phosphate and ammonium from sewage sludge. Hydrothermal treatment could achieve the transformation of all kinds of P species like phosphonate, organic phosphates and polyphosphate mainly into inorganic orthophosphate (Huang and Tang, 2015). Deamination also occurs during hydrothermal treatment, which may produce high concentration of NH_4^+ in the hydrolysate. At mild temperatures below 220 °C, labile organic N can be disintegrated resulting in accelerated ammonium release from waste activated sludge and dewatered anaerobically digested sludge (Bougrier et al., 2008; He et al., 2015). Therefore, hydrothermal treatment is considered as an appropriate pretreatment method of sludge for struvite crystallization. Up to the present, however, little information is available regarding P and N recovery as struvite from sludge after being hydrothermally treated.

The objective of this part was to develop a hybrid process of hydrothermal pretreatment with struvite crystallization to recover P and N from sludge. More specifically, the influence of hydrothermal temperature and residence time on P and N release was first evaluated. Then struvite crystallization process was optimized to recover phosphate and ammonium from the hydrolysate. Finally, characterization of the formed struvite was performed to provide the feasibility of using the precipitates as fertilizer.

3.2 Materials and methods

3.2.1 Sludge sample

The sludge used in this study was anaerobically digested sludge sampled from a wastewater treatment plant in Ibaraki prefecture, Japan, which was kept at 4 °C in the refrigerator prior to use. The sludge was shaken and mixed thoroughly before being

used for experiments. Table 3-1 shows the main characteristics of this sludge. Total P and total N were averagely 4.49% and 7.71% based on total solids (TS), respectively. In addition, the average soluble P and NH_4-N were 373.16 mg/L and 318.80 mg/L in the supernatant.

3.2.2 Hydrothermal treatment

Hydrothermal treatment was conducted in a stainless-steel tube reactor (MMJ-200, OM Labtech Co., Japan) with working volume of 200 mL, the maximum pressure of 20 MPa and maximum temperature of 300 °C, respectively. The reaction pressure was that of water alone at the respective temperature. One hundred and eighty mL of sludge sample was used in each trial. After the sludge being loaded, the hydrothermal reactor was heated to the designated temperature and then kept at this temperature for a designated residence time. A series of runs were performed at different temperatures (120, 140, 160, 180, 200, 220, and 240 °C) to get the maximum amount of phosphate and ammonium release. The residence time was recorded right from the moment that the reactor reached the designated temperature. In this study, four residence times (1 min, 15 min, 30 min, and 60 min) were chosen to test its effect on the dissolution of P- and N- containing substances in the sludge. After the hydrothermal reaction, the reactor was cooled to room temperature by a fan. The hydrolysate (about 168 mL from each run) was separated by vacuum filtration using filter paper (Whatman 1004-055, USA). Detailed properties of the solid residues and gases were not included here, as the major focus of this work was to recover P and N from the hydrolysate. The hydrolysate was also preserved in the refrigerator at 4 °C before being used for subsequent struvite precipitation experiments.

3.2.3 Struvite precipitation

Equimolar concentrations (1:1:1) of magnesium ion (Mg^{2+}), phosphorus ion (PO_4^{3-}) and ammonium ion (NH_4^+) are required to precipitate struvite (Rahaman et al., 2014). struvite can form by precipitation of Mg^{2+}, NH_4^+, and PO_4^{3-} ions if their solubility product is higher than the product (struvite) solubility, i.e. pK_{SP} = 13.26 (Ohlinger et al., 1998). As pH plays an important role in struvite precipitation, the minimum solubility of struvite is reported at approximately pH 9.0 (Buchanan et al., 1994). This study explored the addition of Mg with initial Mg/P molar ratio in the hydrolysate being 1:1,

1.5:1 and 2:1, respectively on struvite precipitation from the hydrolysate at pH 9.0, and 10.00 g/L of $MgCl_2$ was used to supply sufficient Mg^{2+} for struvite precipitation. The experimental procedure was as follows. Firstly, every 50 mL of hydrolysate was added to a 100 mL beaker without mixing. Secondly, different amount of $MgCl_2$ solution was added into the hydrolysate followed by pH adjustment to 9.0 ± 0.1. Finally, the mixture was centrifugalized and filtered through 0.45 μm filter paper after 1 h. The precipitates were air dried naturally and weighed.

In addition, this study also tested the influence of initial pH on struvite precipitation at pH 8.0, 9.0 and 10.0, respectively. In these trials, the $MgCl_2$ solution was firstly added into the hydrolysate, then the mixture pH was adjusted with 5 M NaOH to pH 8.0, 9.0 or 10.0 within 2 min, respectively. After that, the mixture pH was not controlled but monitored during the precipitation process of each trial.

3.2.4 Analytical methods

Orthophosphate, NH_4-N, suspended solids (SS) and volatile suspended solids (VSS) were measured following the standard methods (APHA, 1998). Soluble carbohydrates and proteins were quantified with the Phenol-sulfuric method and the Coomassie brilliant blue method by using Shimadzu UV-1800 (Japan), respectively. Soluble total organic carbon (TOC) was analyzed by a TOC analyzer (Shimadzu TOC-V_{CSN}, Japan). Volatile fatty acids (VFAs) concentrations were determined via Shimadzu GC-8A (Japan) equipped with an insole F-200 30/60 column. Metal ions (Ca, Fe, Al, B, Cd, Cr, Cu, Mg, Mn, Na, Pb, and Zn) in the liquid were analyzed by ICP-OES (Perkin Elmer Optima 7300DV, USA) after the hydrolysate being filtered through 0.22 μm membrane and digested with nitric acid and hydrogen peroxide at 98 °C. pH was monitored using a pH meter (Mettler Toledo, FE20, Switzerland).

The precipitates were characterized by FTIR (JASCO FT/IR -300, Japan) and XRD (BRUKER D2 PHASER, Germany). FTIR data was obtained in the range of 400-4000 cm^{-1}. XRD data were collected with Cu K radiation source over a 2θ angle range of 5-60º in a counting step of 0.02º with an integration time of 0.6 s at 30 kV and 10 mA.

Mg ion and other metal ions in the precipitates were measured after being digested with nitric acid and hydrogen peroxide at 98 °C, and then the ratio of each element (N, P and Mg) in the precipitates were calculated.

3.2.5 Calculation

Hydrothermal treatment was conducted in triplicate, and the obtained hydrolysates were mixed to carry out the subsequent struvite precipitation experiments. All the results were expressed as the mean values of the triplicate tests.

The release efficiencies for P and N from sludge particles during hydrothermal treatment were calculated according to Eq. (3-1).

$$\text{Release efficiency (P or N, \%)} = \frac{\Delta m_s}{m_p} \times 100 = \frac{[C]_{ht} \times V_{ht} - [C]_{s,ads} \times V_{ads}}{([C]_{t,ads} - [C]_{s,ads}) \times V_{ads}} \times 100 \quad (3\text{-}1)$$

where Δm_s (mg) is the mass change of soluble P or N in the liquid phase of sludge after hydrothermal treatment, and m_p (mg) is the mass of particulate P or N in the sludge before hydrothermal treatment. [C] (mg/L) and V (mL) are P or N concentration in the hydrolysate (denoted by lower *ht*) or anaerobically digested sludge (denoted by lower *ads*), and their volume, respectively. The subscript *s* or *t* denotes the soluble or total concentration of P or N in the sampled anaerobic digested sludge. In this work, it was supposed that no significant change occurred in sludge volume after hydrothermal treatment.

The removal efficiencies for P, N, and Mg from the hydrolysate through struvite precipitation were estimated according to Eq. (3-2).

$$\text{Removal efficiency (P, N or Mg, \%)} = \frac{[C]_{i,ht} - [C]_{f,ht}}{[C]_{i,ht}} \times 100 \quad (3\text{-}2)$$

where [C] (mg/L) is the concentration of P, N or Mg in the hydrolysate. The subscripts, *i*, *f*, and *ht* denote initial, final and hydrolysate, respectively.

The purity of struvite (%) in the produced struvite was calculated based on N content in the precipitate according to Eq. (3-3), assuming that all N in the precipitate is only in the form of struvite.

$$\text{Struvite purity (\%)} = \frac{[N]_{prec}}{[N]_{theo}} \times 100 \quad (3\text{-}3)$$

where $[N]_{prec}$ and $[N]_{theo}$ are N mass ratio in the precipitate and theoretical N mass ratio (5.71%) in struvite or $MgNH_4PO_4 \cdot 6H_2O$ (Ohlinger et al., 1998), respectively.

Results and discussion

3.3.1 Optimization of hydrothermal temperature and residence time for P and N release

(1) Hydrothermal temperature

Sewage sludge usually contains complex organic matters like carbohydrates, proteins, lipids, and lignin and mineral materials (Goto et al., 1999). During hydrothermal reaction, organics can be decomposed with minerals including phosphate and ammonium being released. As hydrothermal temperature exhibits more impact on solid organics decomposition than reaction time (Danso-Boateng et al., 2013), the effect of different hydrothermal temperature (from 120 °C to 240 °C with 20 °C intervals for 30 min) on P and N release was firstly explored.

As an indicator of total soluble organics, soluble TOC showed a steady increase with the increase in temperature (Fig. 3-1). Hydrothermal treatment at higher temperature led to a steady decrease in final pH from 6.27 (120 °C) to 5.53 (240 °C). This decrease in hydrolysate pH during hydrothermal reaction of biomass is a typical phenomenon, most probably attributable to the formation of VFAs (Jain et al., 2016), especially acetic acid as shown in Fig. 3-3. Two important intermediates, carbohydrates and proteins were also determined in the hydrolysate. Carbohydrates in the hydrolysate were detected to the first increase from 120 °C to 180 °C and then decrease substantially to 240 °C (Fig.3-4), achieving its highest level of 1591.97 mg/L at 180 °C. This phenomenon is in agreement with the statement made by Yu et al. (2008) who pointed out that more sugars could be recovered from hemicellulose by hydrolysis at a lower temperature, which can be degraded at high temperature. The level of proteins, on the other hand, was determined to decrease with the increase in hydrothermal temperature, possibly because the peptide bond linking amino acids together into proteins is readily hydrolyzed in hydrothermal systems (Peterson et al., 2008). Thus, organic matters seem to be efficiently hydrolyzed during hydrothermal pretreatment.

P speciation in water includes both organophosphorus and inorganic phosphate, while the reactive P for struvite precipitation is limited to orthophosphate (PO_4^{3-}, HPO_4^{2-}, $H_2PO_4^-$). In this work, it was found that TP concentration was approximate to orthophosphate concentration in the hydrolysate. Therefore, only orthophosphate concentration data were used in the following experiments. Fig. 3-2 shows the changes

of orthophosphate and ammonium concentrations in the hydrolysate after hydrothermal treatment at different reaction temperatures. A positive correlation was found between the increase in phosphate and increase in temperature when hydrothermal temperature varied from 120 °C to 200 °C, and the highest concentration of P (579.98 mg-P/L) was obtained at 200 °C. Based on Eq. (3-1), the P release efficiency was about 48.54% under this condition. However, when further increasing the hydrothermal temperature, carbonization phenomenon of sludge was observed, resulting in more mineral precipitates. This observation to a great extent leads to the steadily decreased P concentration from 579.98 mg-P/L to 387.65 mg-P/L when the hydrothermal temperature was further increased to 240 °C.

Meanwhile, ammonium (NH_4) concentration increased from 320.69 mg-N/L to 490.38 mg-N/L with hydrothermal temperature increased from 120 °C to 240 °C as shown in Fig. 3-2. The relatively large increase in NH_4 and decrease in proteins (Fig. 3-4) were observed when temperature > 180°C, which is to some extent in agreement with the results of Wilson and Novak (2008) who performed hydrothermal treatment on bovine serum albumin and found that notable proteins loss occurred at temperature > 170 °C. Ekpo et al. (2016) also noticed that the increase in NH_4-N was only around 120-180 mg/L when swine manure together with deionized water or 0.1 M acetic acid was hydrothermally treated for 1 h as temperature increased from 120 °C to 250 °C. The insignificant improvement in NH_4^+ release might also be attributed to the anaerobically digested sludge used in this work. During anaerobic digestion, most of the biodegradable N-containing organics can be decomposed and converted into NH_4^+, resulting in less further release of NH_4^+ during the followed-up hydrothermal treatment. In this study, taking the effect of temperature on both P and ammonium release during hydrothermal treatment (Fig. 2-2) into consideration, 200 °C was determined as the suitable temperature for NH_4-N release achieving NH_4-N concentration of 456.85 mg/L in the hydrolysate with NH_4-N release efficiency about 13.10% based on Eq. (2-1).

(2) Residence time of hydrothermal treatment

Residence time also plays a significant role in the distribution of different types of products (Jain et al., 2016). This work investigated the effect of residence time (1 min, 15 min, 30 min and 60 min) on P and N release. Results showed that longer residence time ranging from 1 to 30 min could yield high concentrations of P and ammonium.

The concentrations of P and NH_4-N were detected to be the highest, about 579.98 mg-P/L and 456.85 mg-N/L, respectively when the residence time was 30 min. Under this condition, 72.57% of TP and 33.29% of TN in the sludge existed in the form of orthophosphate and ammonium in the hydrolysate, respectively. However, further prolonging of residence time may lead to a decrease in P and ammonium concentrations in the hydrolysate. The concentrations of P and ammonium were found to drop to 410.16 mg-P/L and 413.87 mg-N/L, respectively when the hydrothermal treatment lasted for 60 min. This observation may be attributable to the co-precipitation of P minerals with or without ammonium in the hydrolysate and loss of ammonium due to the easy escape of ammonia formed during hydrothermal treatment for a longer time. In this work, hydrothermal pretreatment at 200 °C for 30 min was considered as the optimal condition for P and ammonium release, from which the hydrolysate was applied for the subsequent struvite crystallization.

3.3.2 Optimization of struvite precipitation

High concentrations of ammonium and P are required for struvite precipitation, resulting in the high recovery of P and N minerals. Besides, increasing the NH_4-N concentration would increase the purity of precipitate (Stratful et al., 2001). Hence, the hydrolysate obtained under 200 °C for 30 min (hydrolysate-200) was used for the struvite precipitation test.

Table 3-2 shows the effect of initial pH on P and NH_4-N removal from the hydrolysate after $MgCl_2$ being added nearly to a molar Mg/P ratio of 1:1. For phosphate, the removal efficiency was increased from 84.61% to 91.60% with pH rose from 8 to 9 based on Eq. (3-2). And at pH 10, the removal efficiency of P was further increased to 95.27%. As stated, small pH variations may lead to instability of the aggregates due to possibly significant change in ζ potential of the particles (Bouropoulos and Koutsoukos, 2000). This observation is almost in consistence with Ma et al. (2014) who claimed that P concentration decreased by 38%, 69% and 100% from a prepared $MgCl_2$-$(NH_4)_2HPO_3$-NaCl-H_2O solution at pH 8, 9 and 10, respectively; and 96%, 99%, and 99% of the removed P were correspondingly detected in the formed struvite. For N removal, a higher NH_4-N removal efficiency was also detected at higher hydrolysate pH. The NH_4-N concentration was detected to decrease by 45.49%, 54.88% and 66.35% at pH 8, 9 and 10, respectively. The above decrease in ammonium concentration might

also be partially contributed by gaseous NH_3 escape due to the increase in hydrolysate pH, as more gaseous NH_3 molecules exist in the hydrolysate at higher pH reflected in Eq. (3-4) (Hansen et al., 1998).

$$Free\ [ammonia - N] = Total\ [ammonium - N]/\{1 + \frac{10^{-pH}}{10^{-\left(0.09018 + \frac{2729.92}{T}\right)}}\} \quad (3\text{-}4)$$

where T(K) is the temperature (Kelvin).

HPO_4^{2-} is the dominant phosphate species in the hydrolysate under slightly alkaline conditions (pH 8-10) (Campbell et al., 2005). During struvite precipitation, pH was observed to decrease to some extent, possibly attributable to the H^+ release during struvite precipitation as follows:

$$Mg^{2+} + NH_4^+ + HPO_4^{2-} \leftrightarrow MgNH_4PO_4 + H^+ \quad (3\text{-}5)$$

In this study, the hydrolysate pH was detected to decrease from initial 8.0, 9.0 and 10.0 to 7.8, 8.9 and 9.7, respectively within the first 1 h, signaling a fast nucleation of struvite crystallization in the hydrolysate.

Even though metal ions can also be released from the sludge to hydrolysate during hydrothermal treatment, Mg concentration in the hydrolysate was only 194.52 mg/L (Table 3-3). Compared with 579.98 mg-P/L of PO_4-P and 456.85 mg-N/L of NH_4-N, the concentration of Mg^{2+} in the hydrolysate is not enough to make an equal molar ratio with phosphate and ammonium. As a result, different amount of Mg^{2+} was added to the hydrolysate. Three Mg/P molar ratios (1:1, 1.5:1 and 2:1) were tested for struvite precipitation at initial pH 9.0 ± 0.1. A significant amount of small white crystals appeared and settled down after $MgCl_2$ being added. The effect of Mg/P ratio on P and N removal are shown in Table 3. The P and NH_4-N removal efficiency increased slightly with the increase in Mg/P ratio from 1:1, 1.5:1, to 2:1, to some extent in agreement with the results from synthetic swine wastewater (Song et al., 2007). The P and NH_4-N removal reached 93.05% and 53.23%, respectively at Mg/P molar ratio around 1 (pH 9.0). In addition, the two batch struvite precipitation tests almost achieved the same P, N, and Mg removals as shown in Tables 2 and 3. A higher Mg^{2+} concentration results in a higher supersaturated index so that struvite can be formed more sufficiently. However, the utilization ratio of Mg or Mg removal from the hydrolysate was detected to decrease sharply from 97.59% to 69.02% with the Mg/P molar ratio increased from 1.0 to 2.0 (Table 3-3). In addition, as shown in Table 2 almost similar Mg removal or utilization (97.59%-97.92%) was realized during struvite precipitation at pH 9.0 and

pH 10.0. Therefore, Mg/P molar ratio of 1 at pH 9 was selected as the optimal condition for struvite precipitation from the hydrolysate in this study.

3.3.3 Mass balance and struvite purity analysis

(1) Mass balance

During struvite precipitation, the mass balance analysis of P, N and Mg was carried out. By summing up the mass of P and Mg in the final hydrolysate and struvite precipitates and then comparing with the corresponding values of the initial hydrolysate, good mass balance was achieved with variance less than 2%. However, the mass of N in the struvite precipitates and the final hydrolysate was less than that in the initial hydrolysate. As previously mentioned, there might be a small part of N that is likely lost during this process. The lost part of N increased with the increase of hydrolysate pH (1.4%, 5.9% and 21.9% at pH 8, 9 and 10, respectively), indicating that N mass would lose a lot at a higher pH value. On the other hand, as shown in Table 2, the mass of precipitates increased with the increase of hydrolysate pH, implying that the metal ions in the hydrolysate are more likely to co-precipitate with phosphate at higher pH like > 9.

(2) Struvite purity from the hydrolysate

The mass ratios of N, P, and Mg and the corresponding purity in the precipitate at different pH conditions are shown in Table 3-4. The struvite purity in the precipitate decreased from 85.81% to 76.18% as pH increased from 8 to 10. It might result from the partial transformation of NH_4^+ into NH_3 gas thus NH_3 volatilization as the hydrolysate pH increased (Song et al., 2007). And a higher pH can easily make Mg^{2+} and Ca^{2+} precipitate with hydroxy. Calcium phosphate and calcium hydroxide might co-exist in the precipitate, as a certain amount of calcium was detected in the solid (Table 3-5). Previous studies found that phosphate removal from struvite precipitation was influenced by the existence of calcium (Capdevielle et al., 2013; Pastor et al., 2008). As known, precipitation of amorphous calcium phosphate on struvite particle surface will affect its further growth. In this study, however, the molar ratio of Ca/Mg was about 0.16 after adding Mg to Mg/P ratio of 1 in the hydrolysate, much lower than the Ca/Mg molar ratio of 0.5 which may inhibit struvite growth (Le Corre et al., 2005).

Therefore, calcium is considered to have a limited impact on struvite precipitation in this study. The ratio of P in the precipitate was higher than the theoretical value, most probably due to the same reason. Other phosphate precipitate like $Ca_3(PO_4)_2$ could also increase the proportion of P in the precipitates.

3.3.4 Characterization of the precipitates by struvite precipitation from the hydrolysate

(1) FTIR spectra

The infrared spectra of the pure struvite sample and precipitates obtained under different initial pH conditions (pH 8, 9 and 10) are shown in Fig. 3-5. The band at 2952 cm^{-1} is the antisymmetric stretching vibration of NH_4 groups. The broad band between 2200 and 2500 cm^{-1} can be assigned to water-phosphate H-bonding (Banks et al., 1975). HOH deformation of water can be observed at 1684 cm^{-1}, and the bands at 1439 and 1460 cm^{-1} are those of the HNH deformation modes of NH_4 (Cahil et al., 2008). The bands of PO_4 units are observed at 1003, 567 and 462 and 438 cm^{-1} (Banks et al., 1975; Suguna et al., 2012). Water-water H-bonding is at 757 cm^{-1}, whereas ammonium-water H-bonding is at 890 cm^{-1} (Banks et al., 1975). The FTIR patterns demonstrate that the precipitates obtained under different initial pH conditions in this study are mainly composed of struvite.

(2) XRD analysis

Fig. 3-6 shows the XRD patterns of pure struvite and the produced struvite crystals in this study. As it can be seen, the prominent peaks of the struvite precipitates match very well with the standard for struvite, implying that orthorhombic struvite is the predominant crystal phase in the produced struvite crystals. Interestingly, the peak intensity of pH 8 struvite precipitate is much stronger than the other two struvite precipitates, most probably attributable to its higher struvite purity as shown in Table 3-4. Although struvite method is limited to qualitatively analyze crystal structure, the peak intensity reflects the contents of struvite in the precipitate to some degree. Therefore, it is interpreted that the precipitates at pH 8 have the highest struvite content, in agreement with the results of Table 3-4 and Hao et al. (2013) results about the effect of pH on struvite precipitation. As a result, a relatively lower pH (pH 8 or pH 9) rather

than higher pH (pH 10) condition can target high-grade struvite crystals in the subsequent struvite precipitation from hydrolysate.

(3) Other metals present in the precipitates

Metal ions, especially hazardous metals, were measured in this study. Results show that except Mg, Ca was found in the maximum amount in the precipitates, about 1.88%, 2.06%, and 2.71% after struvite precipitation at pH 8, 9 and 10, respectively. It is speculated that calcium hydroxide might be the small quantity of calcium deposited in the precipitates. As it can be seen from Table 3-5, the effect of Ca^{2+} on struvite precipitation was very limited in this study in spite of its relatively high concentration (70.17 mg/L) in the hydrolysate of sludge after being hydrothermally treated at 200°C for 30 min.

Heavy metals in the precipitates are very sensitive if the produced struvite being used as fertilizer. Although Cu, Cr, Mn, and Pb were all detected in the hydrolysate, little was determined in the produced precipitates. All the concentrations of tested heavy metals meet the US EPA standards for land application. This observation indicates that the precipitates formed from the hydrolysate are safe to be used as fertilizer. Compared with direct struvite precipitation from anaerobically digested sludge or digested sludge liquor, it is much safer by using the hydrolysate, most probably due to the fact that heavy metals have been immobilized in the solid phase during hydrothermal treatment process (Shi et al., 2013; Wang et al., 2016).

3.4 Summary

In order to dispose excess sewage sludge and recycle its nitrogen and phosphorus resources, hydrothermal pretreatment coupling with (struvite) crystallization was investigated. Hydrothermal pretreatment at different temperature and residence time were performed on anaerobically digested sludge to maximize phosphate and ammonium release and their recovery from the resultant hydrolysate. Results showed that hydrothermal pretreatment at 200 °C for 30 min favored phosphate and ammonium release achieving phosphate and ammonium concentrations at 579.98 mg-P/L and 456.85 mg-N/L, respectively. During the subsequent struvite precipitation, the optimum condition for N and P recovery was determined at pH 9 and Mg/P molar ratio of 1, realizing P and N recovery of 91.60% and 54.88% respectively from the hydrolysate in

addition to struvite purity of 84.24%. The produced struvite was also confirmed by FTIR and XRD analysis.

Tables

Table 3-1 Main physicochemical characteristics of anaerobically digested sludge used in the experiments.

Parameters	Sewage sludge	Unit
Total solids (TS)	1.78	%
Volatile solids (VS)	81.56	% of TS
Carbon	37.84	% (dw)
Hydrogen	7.06	% (dw)
Nitrogen	7.71	% (dw)
Phosphorus	4.49	% (dw)
pH	6.30	

dw, dry weight of the sludge

Table 3-2 Effect of initial pH on P and NH_4-N removal from hydrolysate after $MgCl_2$ being added to a molar Mg/P ratio of 1:1.

	Initial pH	Final pH	Final P in hydrolysate (mg/L)	P removal (%)	Final NH_4-N in hydrolysate (mg/L)	NH_4-N removal (%)	Final Mg in hydrolysate (mg/L)	Mg removal (%)	Mass of precipitates (mg/L)
Initial	5.92	-	579.98	-	456.85	-	451.51*	-	
pH 8	8.00	7.79	89.26	84.61	249.01	45.49	59.20	86.89	4110
pH 9	9.00	8.87	48.73	91.60	206.11	54.88	10.89	97.59	4655
pH 10	10.00	9.68	27.43	95.27	153.74	66.35	9.38	97.92	4665

* The initial Mg concentration was measured after $MgCl_2$ addition.

Table 3-3 Effect of increase in Mg/P molar ratio on P and NH_4-N removal after 1 h struvite precipitation at an initial pH of 9.0.

Tested condition	Initial Mg (mg/L)	Final Mg (mg/L)	Mg removal (%)	Final P (mg/L)	P removal (%)	Final NH_4-N (mg/L)	NH_4-N removal (%)
Initial hydrolysate	194.52	-	-	579.98	-	456.85	-
Mg: P=1:1	451.51	10.89	97.59	40.29	93.05	213.69	53.23
Mg: P=1.5:1	675.24	141.40	79.06	23.11	96.02	203.84	55.38
Mg: P=2:1	890.99	276.00	69.02	22.41	96.14	198.06	56.65

The Mg/P ratios in these experiments were the actually initial molar ratios of Mg/P in the tested hydrolysate for struvite precipitation.

Table 3-4 Comparison of produced struvite purity and its component mass changes at different initial pHs.

Initial pH	Mass ratio detected in the precipitate (%)			struvite purity in the precipitate (%)[a]	struvite amount (mg/L)	Struvite mass ratio of each component in the precipitate (%) [b]		
	N	P	Mg			N	P	Mg
8	4.90	11.03	9.21	85.81	3527	85.81	98.18	92.24
9	4.81	11.30	9.37	84.24	3921	84.24	94.08	89.00
10	4.35	11.72	9.41	76.18	3554	76.18	82.03	80.15

Theoretical mass percentages of N, P and Mg in struvite are 5.71%, 12.62% and 9.90%, respectively (Ohlinger et al., 1998)

[a] The struvite purity is calculated according to the mass of N in the formed precipitate and the assumption that all N in the precipitate are only in the form of struvite.

[b] Struvite mass ratio is calculated as the percentage of the mass of each component in struvite to that of the total precipitate.

Table 3-5 Main metals detected in the hydrolysate of sludge after being hydrothermally treated at 200 °C for 30 min and the struvite precipitates formed in 1 h at different initial pHs.

Element	Hydrolysate -200 (mg/L)	Precipitates at pH 8 (mg/g)	Precipitates at pH 9 (mg/g)	Precipitates at pH 10 (mg/g)	US EPA Standard (mg/g)
Ca	70.17	1.88	2.06	2.71	-
Fe	27.27	0.21	0.33	0.39	-
Al	1.23	0.08	0.09	0.06	-
B	6.68	0.13	0.07	0.11	-
Cd	0.00	0.00	0.00	0.00	0.04
Cr	0.12	0.00	0.01	0.01	3
Cu	2.89	0.06	0.04	0.06	4.3
Mg	194.52	92.13	93.67	94.08	-
Mn	0.68	0.03	0.07	0.05	-
Pb	0.00	0.00	0.00	0.00	0.84
Zn	0.44	0.00	0.01	0.00	7.5

Figures

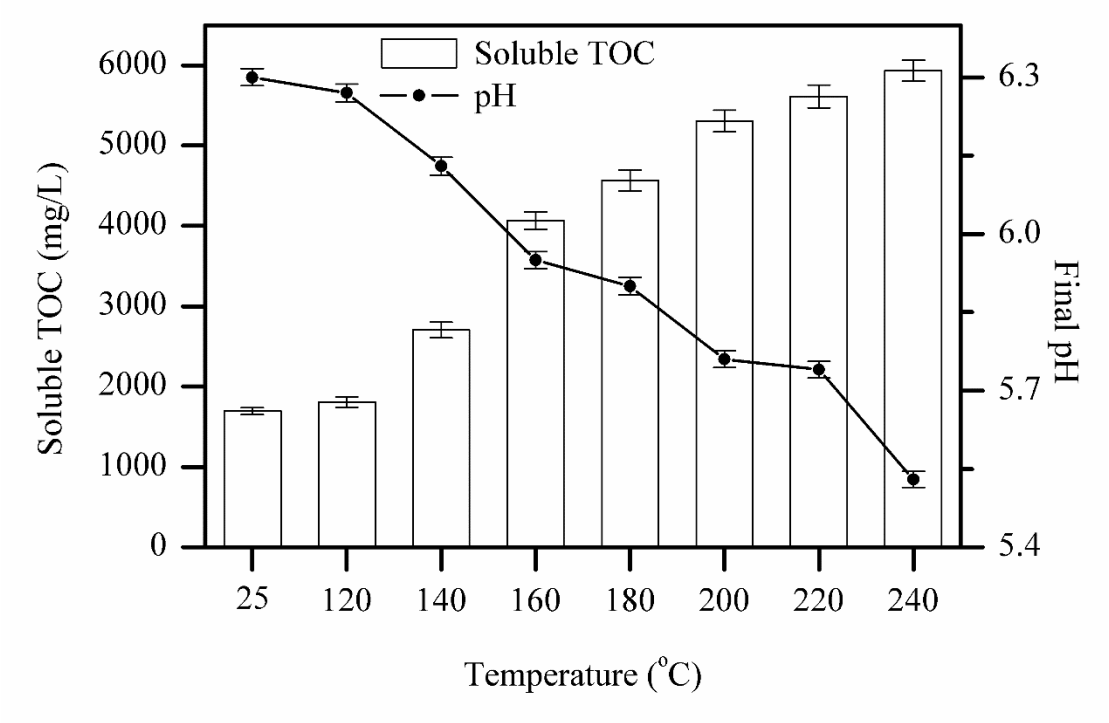

Fig. 3-1 Changes in soluble total organic carbon (TOC) and final pH in sludge after being hydrothermally treated for 30 min at different temperatures.

Soluble TOC and pH at 25 °C were determined in the supernatants of sampled sludge after centrifugation at 9000 rpm for 10 min.

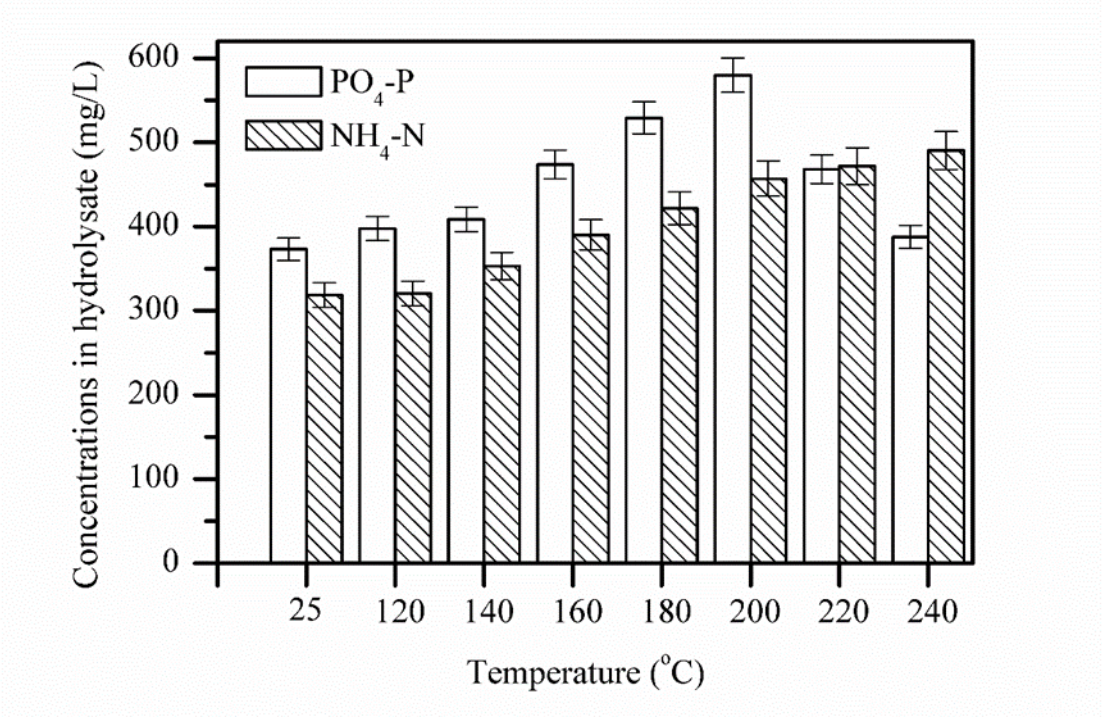

Fig. 3-2 Phosphate and ammonium release from sludge into the hydrolysate after hydrothermal treatment at different temperatures.

The concentrations of phosphate and ammonium at 25 °C were determined in the supernatants of sampled sludge after centrifugation at 9000 rpm for 10 min.

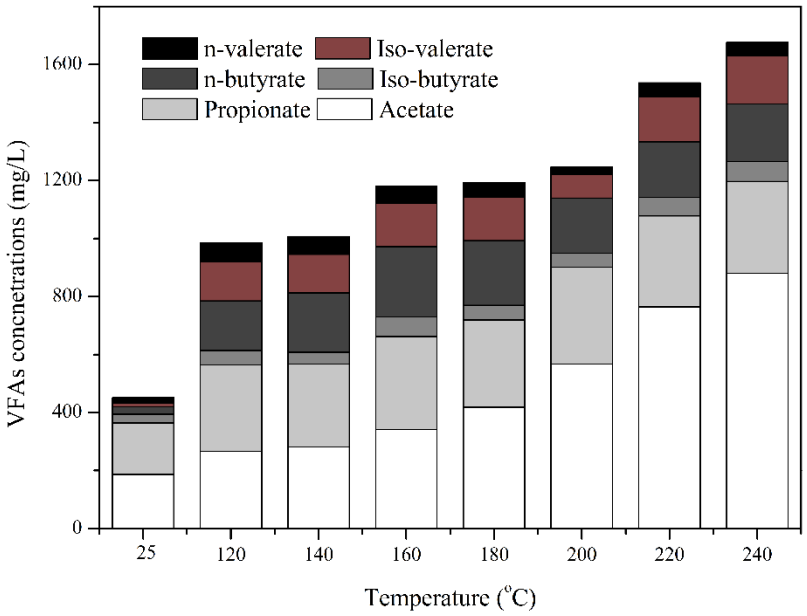

Fig. 3-3 Effect of hydrothermal pretreatment temperature on volatile fatty acids (VFAs) production.

VFAs concentration at 25 °C was determined in the supernatants of sampled sludge right after centrifugation at 9000 rpm for 10 min.

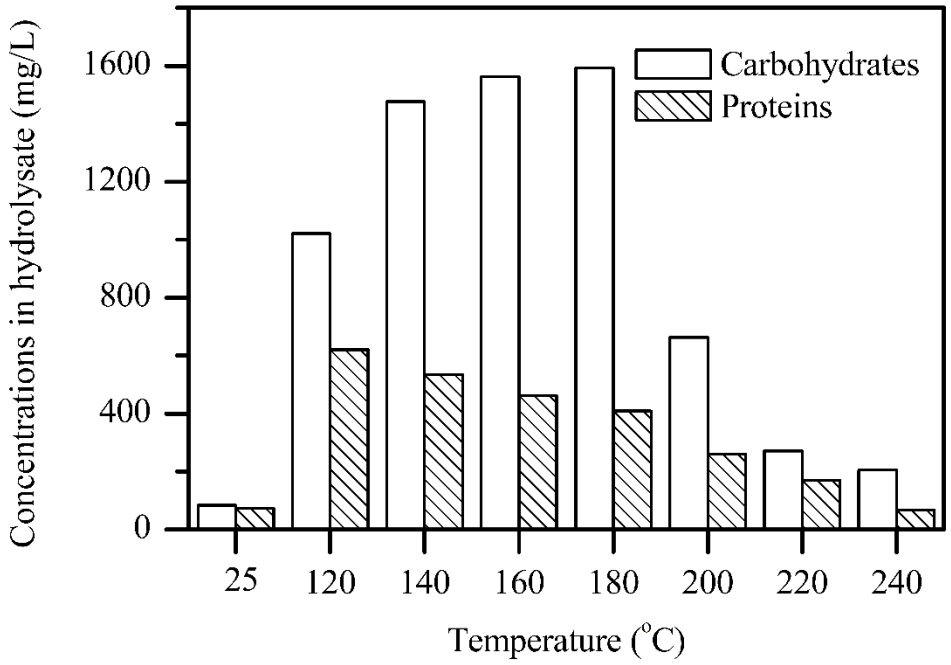

Fig. 3-4 Effect of hydrothermal pretreatment temperature on soluble carbohydrates and proteins.

The concentration of carbohydrates and proteins at 25 °C were determined in the supernatants of sampled sludge right after centrifugation at 9000 rpm for 10 min.

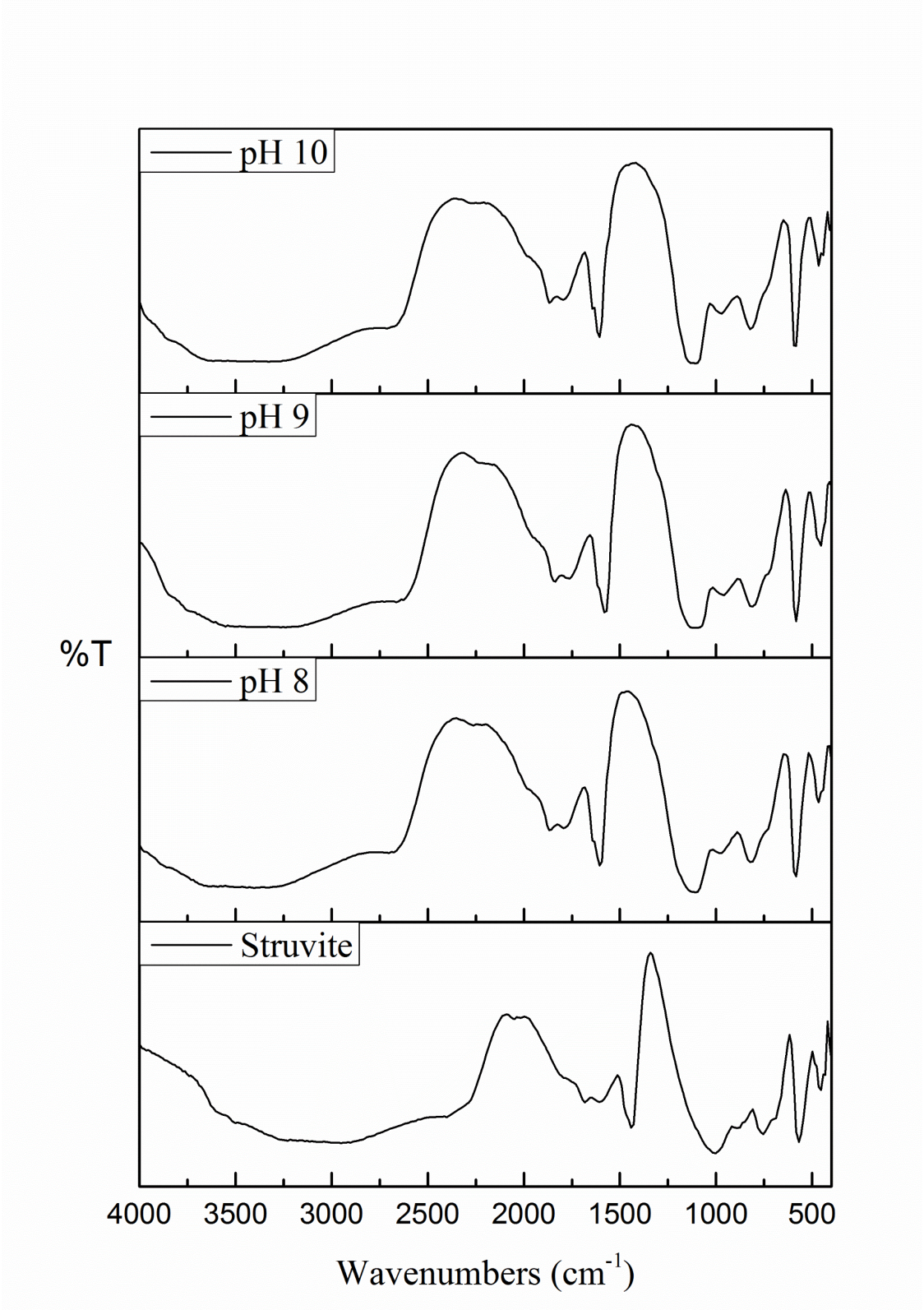

Fig. 3- 5 FTIR spectra of the struvite standard and struvite precipitates at pH 8, 9 and 10, respectively.

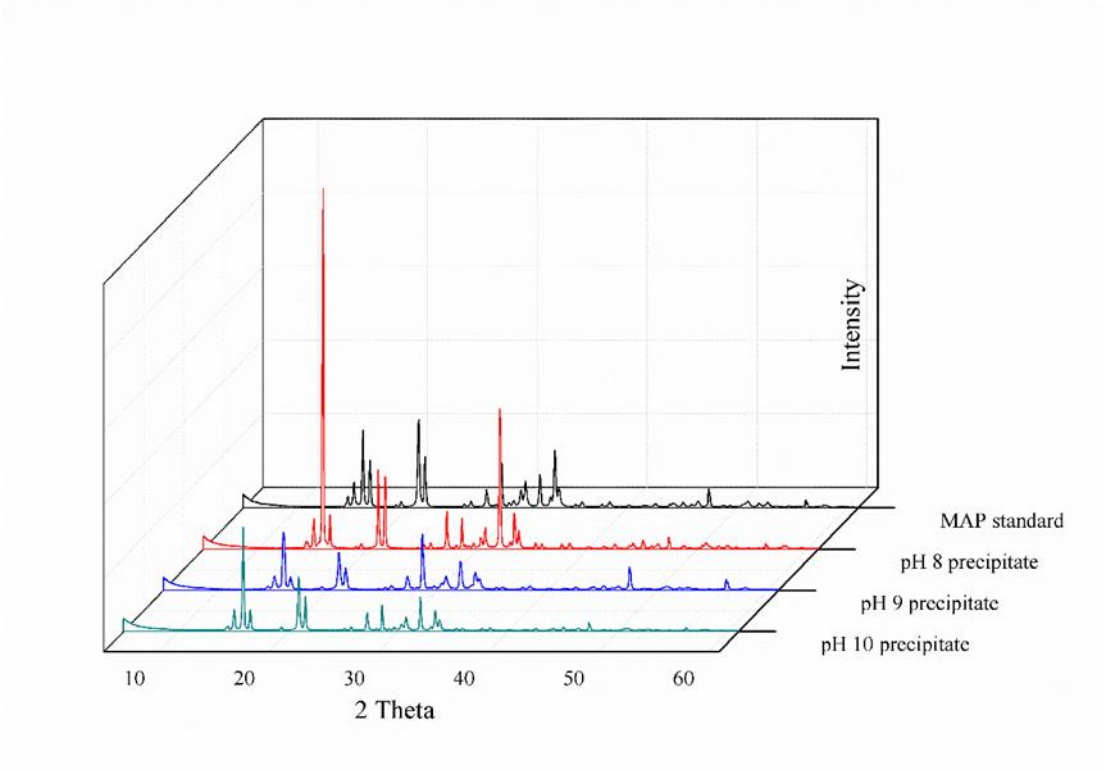

Fig. 3- 6 XRD patterns of the struvite standard and the precipitates formed in 30 min at pH 8, 9 and 10, respectively.

Chapter 4 Hydrothermal carbonization of anaerobic granular sludge: the potential application of hydrochars

4.1 Introduction

Recently anaerobic granular sludge (AGS) technology has been applied worldwide in upflow anaerobic sludge blanket (UASB) and expanded granular sludge bed (EGSB) systems to treat high-strength organic wastewaters. This biotechnology has demonstrated its incomparable advantages of high loading rate, easy solid-liquid separation and low energy consumption in numerous practical applications (McHugh et al., 2003). However, there were still few detailed reports on energy and nutrients recovery from AGS.

AGS possesses several potential advantages over the conventional sewage sludge for hydrochar production. Firstly, AGS itself has a characteristic of excellent settleability (Alphenaar, 1994). As it is known, the heat capacity of water is very high so that it takes too much energy to remove the moisture inside the sludge with less hydrochar production. Therefore, AGS rather than sewage sludge is expected to save a lot of energy when being used for hydrochar production. Secondly, AGS contains various microorganisms which mainly consists of proteins, carbohydrates and lipids. The HHV of hydrochar could further be increased through the dehydration and decarboxylation reactions during HTT (Danso-Boateng et al., 2013; Peterson et al., 2008). At last, the disintegration of various organics into inorganic substances is considered beneficial for enhancement of nutrients (N and P) availability in the produced hydrochar. Thus AGS-based hydrochar is prospected as an excellent energy carrier and fertilizer, and the hydrolysate produced by HTT of AGS can be used to adjust the organic loading rate of UASB reactor due to lots of organics contained.

This chapter investigated the hydrothermal treatment of AGS. The mass balance in the HTT products, e.g. hydrochar and hydrolysate was analyzed. The physical, chemical and thermal properties of the hydrochar were systematically characterized. In addition, the feasibility of the hydrochar being as fuels and fertilizers was evaluated as well. Fig.4-1 illustrates the energy and resources recovery process based on HTC of AGS.

4.2 Materials and methods

4.2.1 Materials

AGS used in this study was sampled from Asahi Beer Brewery in Ibaraki Prefecture, Japan. The supernatant liquor was discarded and the remaining AGS was kept in the refrigerator at 4 °C prior to use for the HTT test. In order to find out the effect of particle size and morphology on hydrothermal products, the AGS was also smashed into slurry using a disintegrator (Zojirushi BM-RS08, Japan) and used as a comparison. Table 4-1 lists the main physicochemical characteristics of the AGS used in this chapter.

4.2.2 Hydrothermal carbonization of AGS

A stainless-steel cylindrical reactor (MMJ-200, OM Labtech Co., Japan) with a working volume of 200 mL was used to perform the HTT of AGS. For each run, 180 g of sludge was dosed into the reactor. Both smashed and raw AGS were used as raw material for HTT test. After the material was loaded, the hydrothermal reactor was heated to the designated temperature (160, 200 and 240 °C) by using a cylindrical electric heating jacket. The reaction pressure was that of water alone at the respective temperature, which ranged from 1 to 4 MPa. The operation temperature was maintained within ±4 °C of the set temperature, with an operation duration of 1 h. After the reaction, the reactor was cooled down with an electric fan to ambient temperature. The solid part (hydrochar) and the liquid part (hydrolysate) were separated by centrifugation at 9000 rpm for 10 min followed by vacuum filtration using filter paper (Whatman 1004-055, USA). The hydrolysate was preserved in the refrigerator at 4 °C before being analyzed. The obtained hydrochar was washed with deionized water until the deionized water turned colorless. After being dried at 60 °C for 2 days, the hydrochar was ground into fine powders and then stored in enclosed plastic bags until analysis.

4.2.3 Hydrolysate analysis

Soluble TOC in the hydrolysate was analyzed by a TOC analyzer (Shimadzu TOC-V_{CSN}, Japan) after being filtered through 0.22 μm membrane (PTFE, Membrane Solutions, US). TP, TN and TAN were measured in accordance with the standard methods. Soluble carbohydrates and proteins in hydrolysate were determined with the Phenol-sulfuric method and the Coomassie brilliant blue method, respectively by using

the spectrophotometer (Shimadzu UV-1800, Japan), respectively. VFAs were quantified by gas chromatography (GC; Shimadzu GC-14B, Japan). pH was determined with a pH meter (Mettler Toledo FE20, Switzerland).

4.2.4 Hydrochar characterization

For the solid analysis, the contents of organic C, H and N in the AGS and the hydrochars were determined by an elemental analyzer (PerkinElmer 2004 CHN, USA), with the organic oxygen content obtained in this study by subtracting C, H, N and ash contents from the total. The metal contents in the hydrochars were quantified using ICPS (Shimadzu ICPS-8100, Japan) after being completely digested with nitric acid and hydrogen peroxide at 120 °C.

P fractionation of the hydrochar samples was performed by using the SMT procedure (Ruban et al., 1999). The result from the SMT procedure can provide an essential evaluation for P bioavailability ((NAIP+OP)/TP) of the hydrochar.

The morphological images of the hydrochar were characterized with SEM (SHIMADZU SSX-550, Japan). The surface area and pore size of the hydrochar were measured by a Quantasorb model surface area analyzer (Quantachrome, QUADRASORB SI USA). The specific surface area was calculated by the BET method, and the pore size distribution in the hydrochar was based on Barret-Joyner-Halenda (BJH) mode. The hydrochar was also characterized by FTIR spectroscopy using KBr pellets in the range of 4000-400 cm^{-1} (JASCO FT/IR-300, Japan). All experiments were performed in triplicate. Data were expressed as the mean ± standard deviation (SD) for all the above tests.

4.2.5 Energy calculation

To evaluate the profitability and feasibility of HTT of AGS, the energy assessment was conducted. The energy required for HTT of AGS was calculated according to Mau and Gross (Mau & Gross, 2017):

$$Q_{input} = [m_w(H_{w,HT} - H_{w,25}) + m_s c_p(T_{HT}\text{-}25)]/m_s \quad (4\text{-}1)$$

where Q_{input} (MJ/kg) is the energy input during HTT; m_w (kg) and m_s (kg) are the contents of liquid part and solid part of AGS. The ambient temperature was 25 °C and the weight loss of AGS was ignored in this study. $H_{w,HT}$ and $H_{w,25}$ are the enthalpy of water at the final hydrothermal temperature and at 25 °C, respectively; c_p is the specific heat capacity

of dry feedstock, 0.0014 MJ/kg °C according to a previous study (Ahn et al., 2009). T_{HT} is the designated hydrothermal temperature.

The higher heating value (HHV) was calculated using an empirical formula (Phichai et al., 2013):

$$HHV = 0.3383C + 1.422(H - O/8) \quad (4\text{-}2)$$

where HHV is calculated by dry-ash-free-basis in MJ/kg. C, H or O (%) is the organic element percentage in the hydrochar. In addition, the Van Krevelen diagram was plotted using the atomic ratios of O/C and H/C in the hydrochar.

Energy densification was expressed as (Makela et al., 2016):

$$\text{Energy densification} = HHV_{hc}/HHV_f \quad (4\text{-}3)$$

where HHV_{hc} and HHV_f are the heating values of hydrochar and feedstock, respectively.

The energy output Q_{output} (MJ/kg) was calculated as

$$Q_{output} = m_{hc} \times HHV \quad (4\text{-}4)$$

where m_{hc} (kg) is the content of hydrochar produced from HTT.

The net energy output was calculated using the following equation (4-5).

$$Q_{net} = Q_{output} - Q_{input} \quad (4\text{-}5)$$

Hydrochar yield was obtained by Equation (4-6).

$$\text{Hydrochar yield (\%)} = 100 \times m_{hc}/m_{AGS} \quad (4\text{-}6)$$

where m_{AGS} (kg) is the content of AGS used in each trail, 0.1724 kg in this study.

4.3 Results and discussion

4.3.1 Effect of HTT on organics transformation

For the raw AGS, the total solid (TS) concentration is higher than the traditional anaerobically digested sludge (～3%) (Manara and Fullana, 2012), about 9.58% in addition to a high volatile solids (VS) content (84.59% of TS) in this study. The organics, especially proteins, carbohydrates and VFAs can be released into the hydrolysates during the hydrothermal treatment. The changes of soluble proteins and carbohydrates in the hydrolysate are shown in Fig. 4-2. In the supernatant of AGS, the concentrations of proteins and carbohydrates were 24.23 and 200.53 mg/L, respectively. While their concentrations increased to 881.43 and 5036.05 mg/L, respectively after HTC at 160 ºC. A further increase in hydrothermal temperature led to the decrease in the concentrations of soluble proteins and carbohydrates, which is similar to the findings by using traditional anaerobically digested sludge in Chapter 3. Carbohydrates can be

decomposed rapidly when the temperature is above 200 ºC (Yu et al., 2008). For proteins, the hydrolysis of peptide bond during HTC can decompose proteins and produce amino acids (Peterson. et al., 2008). Results from this work show that the release amount of proteins and carbohydrates from AGS is much higher than that from traditionally anaerobically digested sludge. This observation might be associated with the fact that the AGS used in this study contained a higher organic matter content (VS content) which mainly consists of proteins and carbohydrates.

Hydrothermal treatment also leads to a remarkable increase in VFAs concentration in the hydrolysate. As shown in Fig. 4-2b, the total VFAs showed a steady increase from 454.31 mg/L to 2557.68 mg/L with the increase in HTC temperature from 160 ºC to 240 ºC. More specifically, HAc is the major VFA species, occupying 67%, 86% and 81% of the total VFAs when HTC was conducted at 160, 200 and 240 ºC, respectively. This observation is in agreement with the finding by Shanableh et al (2000) who hydrothermally treated the secondary activated sludge after being thickened. As an important intermediate in anaerobic digestion, HAc-rich hydrolysate can be recycled and used for methane production and/or AGS cultivation.

On the other hand, the soluble TOC concentration increased from 1118.80 mg/L in the supernatant of the raw AGS to 15611.11mg/L in its hydrolysate after HTC at 160 ºC, which kept rising as the temperature was increased from 160 ºC to 200 ºC. As shown in Fig. 4-3a, the C percentage in the liquid phase varied from 37% (at 160 ºC) to 62% (at 240 ºC). Compared to the results (20-37% in the liquid phase) obtained by Berge et al. (2011), a larger proportion of C was transferred into the liquid probably due to the high VS content in the AGS used in this study. Hydrolysis of the organics and Maillard reaction may be responsible for this phenomenon (Zhuang et al., 2017). A detailed mass balance of C, N and P in the HTC products are shown in Table 4-2.

4.3.2 Effect of HTT on P and N

The P distribution before and after HTC are shown in Fig. 4-3b. As for the raw AGS, OP, NAIP and AP occupied 2%, 77% and 21% of TP, respectively. In this study, P was found to mostly remain in the hydrochar after HTC, and only a little increase of P concentration was detected in the liquid phase, from 3% to 5% as the HTC temperature was increased from 160 ºC to 240 ºC.

For the P fractions in the hydrochar, NAIP was the major one, accounting for 81%, 83% and 88% after HTC at 160, 200 and 240 ºC, respectively. In the meantime, AP content decreased to 16%, 14% and 8%, correspondingly. The contents of metals were

also determined in order to explain why NAIP was the major fraction in the hydrochars (Table 4-3). Al, the main metal ion in the raw AGS, together with phosphates exists as the form of NAIP. The raw AGS contained about 5 mg/g of Al which increased to around 8, 16 and 21 mg/g in the hydrochar-160, hydrochar-200 and hydrochar-240, respectively, due to the decomposition of organics and a large decrease in solid weight (TS). Other metals like Mg, Fe and Zn in the hydrochar showed the same trend as Al, which can also combine with P in the form of NAIP. Ca was the second highest content metal in the AGS, contributing to a small portion of AP in the hydrochar. Compared with other P fractions, AP is difficult to be utilized by plants and microorganisms (Ruban. et al., 1999). The AGS-based hydrochar containing a highly bioavailable P (especially NAIP) content reflects a high potential for being used as a P fertilizer.

In contrast to P, N tended to release into the hydrolysate during hydrothermal treatment. N distribution in the solid decreased from 45.36% to 17.61% with the increased in HTC temperature from 160 °C to 240 °C. The N content in the solid decreased accordingly from ~ 10% in AGS to 8%, 7% and 5% at 160, 200 and 240 ºC, respectively (Fig. 4-3c). This observation is consistent with the results of organics release, which is similar to the hydrothermal treatment of traditional sewage sludge (Danso-Boateng et al., 2015). More importantly, the N component in fuels will be transformed into NO_X during the combustion process. As a consequence, N reduction in hydrochar is beneficial for a reduction in NO_X emission when the hydrochar serves as an energy carrier.

Compared to the raw AGS, the smashed AGS showed a higher dissolution amount of C, P and N during HTC. The P concentration in its hydrolysate was above 500 mg/L, much higher than that from the raw AGS. C and N showed a less variation tendency than P. A detailed comparison between the raw (unbroken) AGS and the smashed AGS on nutrients release is shown in Table 4-4. Generally, the nutrients in the smashed AGS tended to release more into the liquid than those in the unbroken AGS, indicating that the granule shape may help entrap the nutrients into the hydrochar after HTC.

4.3.3 Elemental composition and higher heating value of hydrochar

Table 4-5 lists the elemental composition and the HHVs of hydrochars. A slight variance in elemental composition was observed in the produced hydrochars. The percentage of C increased from ~ 44% in the raw AGS to 45%, 46% and 50% in the hydrochars after HTC at 160, 200 and 240 ºC, respectively. Meanwhile, the percentage

of N showed an opposite trend, reaching to the lowest, about 5.49% in the hydrochar processed at 240 ºC.

On the other hand, the increase in HTC temperature showed a positive effect on the HHVs of the produced hydrochars, about 19.93, 21.65 and 24.01 MJ/kg for hydrochar-160, hydrochar-200 and hydrochar-240, respectively. The HHV of hydrochar-240 is higher than those derived from primary sewage sludge (17-19 MJ/kg) (Danso-Boateng et al., 2015), activated sludge (18.82-20.17 MJ/kg) Zhao et al., 2014) and anaerobically digested sludge (around 15 MJ/kg) (He et al., 2013) obtained under the similar hydrothermal conditions. The energy densification factors of the produced hydrochars ranged from 1.01 – 1.21. However, the hydrochar yield decreased markedly with the increase in HTC temperature. As shown in Table 4-5, the maximum hydrochar yield of 62% was obtained at 160 ºC, which was about 32% and 23% when HTC was performed at 200 ºC and 240 ºC, respectively due to the enhancement of decomposition of solid organics at higher temperatures. This observation agrees with a previous work on HTC of dairy manure (Wu et al., 2017). More specifically, the only difference between the HTC of AGS and other organic wastes is that a larger decrease in hydrochar yield was achieved along with the increase in HTC temperature (this work), most probably due to the high content of decomposable organics in the AGS used in this study. The ash content in the hydrochar, on the other hand, increased with the increase in HTC temperature, from ~15% of the raw AGS to 16%, 22% and 26% when the HTC was operated at 160, 200 and 240 ºC, respectively.

The van Krevelen diagram plotted by the atomic ratios of H/C and O/C is shown in Fig. 4-4. The results indicate that, with the increase in HTC temperature, the H/C and O/C atomic ratios decreased linearly, suggesting that dehydration and decarboxylation reactions might occur during the HTC of AGS (Wu et al., 2017).

In order to analyze the energy balance, the input and output of the energy were calculated (Table 4-5). As expected, the input energy increased with the increase in HTC temperature. Meanwhile, partially due to the decline in hydrochar yield, the output energy decreased with the increase in HTC temperature. The hydrochar yield was about 63%, 43% and 32% when the HTC was operated at 160, 200 and 240 ºC, respectively. The net energy output for hydrochar-160 was 6.86 MJ/kg, which dropped to 2.19 and -0.99 MJ/kg for hydrochar-200 and hydrochar-240, respectively. This observation suggests that a higher-temperature HTC is not suitable for AGS treatment targeting energy recovery due to a much lower hydrochar yield, although the HHV of the resultant hydrochar increased to some extent.

4.3.4 Additional properties for the hydrochar

(1) Thermal analysis of the raw AGS and produced hydrochars

To better understand the combustion characteristics of the hydrochars, the DTA/TG/DTG analysis was conducted (Fig. 4-5). As for the oven-dried raw AGS, three major weight loss steps were observed. The first peak appeared at around 200 °C for the DTG curve, due to the dehydration and devolatilization processes. The next weight loss occurred between 240 °C and 500 °C, attributable to the combustion of organic matters. When the temperature > 550 °C, the weight loss was mainly related to the inorganic matters. For the hydrochars, the first weight loss step was observed at around 300 °C, most probably due to the combustion of organic matters. However, a new weight loss step was noticed at 450 °C, owing to the combustion of the fixed carbon. For the hydrochars produced at 160 °C and 200 °C, the peak at 450 °C was not so obvious, implying that the AGS was not completely carbonized under the tested conditions. Moreover, the fluctuations in the plots resulted from the combustion of organics. Specifically, for the hydrochar produced at 240 °C, its DTG curve showed two obvious peaks at 300 °C and 450 °C, respectively, indicative of the related exothermic reactions confirmed by its DTA curve. This phenomenon is similar to the sewage sludge-derived hydrochar obtained by He et al. (2013).

(2) FTIR analysis

The FTIR analysis was performed to understand the changes in functional groups in hydrochars obtained at different HTC temperatures (Fig. 4-6). The HTC temperature seemed to have limited influence on the functional groups of the produced hydrochars. The band between 3400 and 3200 cm^{-1} attributable to -OH stretching vibration in hydroxyl or carboxyl groups became weaker as the HTC temperature increased. This observation might be resulted from the dehydration of AGS, agreeing with the finding from the van Krevelen diagram. The band between 3000 and 2800 cm^{-1} can be ascribed to the C–H bonds from methyl and methylene groups (de Oliveira et al., 2012). In the spectra of hydrochar-160 and hydrochar-200, the band at 1540 cm^{-1} was noticed, which is attributable to the asymmetric stretching of -C=O in carboxylic groups (Li et al., 2011). Whereas in the spectra of hydrochar-240, no band at 1540 cm^{-1} was detected, indicating that the decarboxylation reactions occurred at a higher HTC temperature like 240 °C.

4.4 Summary

Hydrothermal carbonization (HTC) of anaerobic granular sludge (AGS) was evaluated for nutrients and energy recovery potentials from hydrothermal products. The rise of C and decline of N contents in the produced hydrochar along with the increase in HTC temperature resulted in its higher heating value (HHV) and less NOx emission when being applied for fuel. However, from the viewpoint of energy balance, low-temperature HTC is more economical because the hydrochar yield decreased sharply at higher temperatures. The net energy output was 6.86 MJ/kg for the hydrochar produced from AGS at 160 ºC, while a negative net energy output was gained at higher temperatures.

With the increase in HTC temperature from 160 ºC to 240 ºC, the concentrations of C and N increased in the hydrolysate. The HTC temperature exerted a limited effect on P distribution. After HTC, only 2.5 - 4.9% of P remained in the hydrolysate; the majority of P, however, were contained in the produced hydrochar, most of which (above 80%) were bioavailable. This result also suggests the great potential of hydrochar being used as P fertilizers.

Tables

Table 4-1 Main characteristics of raw AGS used in this study

Parameter (unit)	Raw AGS	Unit
Total solids (TS)	9.58±0.18	%
Volatile solids (VS)	84.59±0.20	% of TS
Carbon (C)	43.79±0.21	% of TS
Hydrogen (H)	6.58±0.19	% of TS
Nitrogen (N)	9.58±0.20	% of TS
Total phosphorus (TP)	122.09±0.89	mg/g-TS
Organic phosphorus (OP)	3.64±0.42	mg/g-TS
Inorganic phosphorus (IP)	118.45±0.80	mg/g-TS
Apatite phosphorus (AP)	24.90±0.45	mg/g-TS
Non-apatite inorganic phosphorus (NAIP)	93.55±0.43	mg/g-TS
pH value	6.80±0.03	

All data were expressed as mean ± SD of triplicate tests.

Table 4-2 Carbon and phosphorus and nitrogen distributions in HTC products of AGS at various hydrothermal temperature

Mass balance was calculated based on 180 mL of anaerobic granular sludge.

HTC temperature (°C)	Carbon distribution			Phosphorus distribution			Nitrogen distribution		
	Solids (g)	Liquid (g)	Deviation* (g)	Solids (g)	Liquid (g)	Deviation (g)	Solids (g)	Liquid (g)	Deviation (g)
raw	7.55	0.20	0.00	2.07	0.04	0.00	1.65	0.28	0.00
160	4.77	2.81	0.17	1.94	0.05	0.11	0.83	1.00	0.10
200	3.43	3.94	0.38	1.92	0.07	0.11	0.52	1.29	0.03
240	2.79	4.46	0.50	1.91	0.10	0.10	0.31	1.45	0.05

* Deviation was calculated as the difference value between the amount of C (N or P) in raw AGS and the amount in the hydrothermal products.

Table 4-3 Main metals detected in the raw AGS and hydrochar of AGS after being HTT at 160, 200 and 240 ºC, respectively.

Sample	Metals content (mg/g)						
	Mg	Al	Ca	Fe	Cu	Zn	Pb
Raw-AGS	0.8030	5.0762	2.0078	0.5896	0.2010	1.2587	0.0000
AGS-160	1.0105	8.1522	2.9457	0.9102	0.3009	2.1132	0.0000
AGS-200	2.3839	15.8380	5.6873	1.4545	0.6276	3.8010	0.0087
AGS-240	2.8823	21.1312	7.9019	2.4082	0.8785	4.9328	0.0113

Table 4-4 A comparison between unbroken AGS and smashed AGS on nutrients release during HTT. (unit: mg/L)

Nutrients	AGS supernatant	Smashed AGS supernatant	Hydrolysate-160	Hydrolysate-S160	Hydrolysate-200	Hydrolysate-S200	Hydrolysate-240	Hydrolysate-S240
C	1118.8	1206.01	15611.11	17103.82	21839.65	29178.3	24777.78	30439.11
N	1576.34	1703.15	5436.56	6350.98	7146.13	8638.76	8075.52	9651.82
P	190.92	197.52	275.07	500.80	362.39	595.77	525.49	548.28

Hydrolysate-Sxx denotes that the smashed AGS was used for HTT.

Table 4-5 Proximate and ultimate analyses of hydrochar (%, TS based)

Samples	C (%)	H (%)	N (%)	O (%)	Hydrochar yield (%)	Ash content (%)	HHV (MJ/kg)	Q_{input} (MJ/kg)	Q_{output} (MJ/kg)	Q_{net} (MJ/kg)
Raw AGS	43.79	6.58	9.58	24.64	-	15.41	19.79	-	19.78	-
Hydrochar-160	44.56	6.51	7.78	24.77	62.11	16.38	19.93	5.52	12.38	6.86
Hydrochar-200	46.16	6.55	6.99	18.46	43.15	21.84	21.65	7.15	6.98	2.19
Hydrochar-240	49.81	6.55	5.49	12.10	32.42	26.05	24.01	8.78	5.42	-0.99

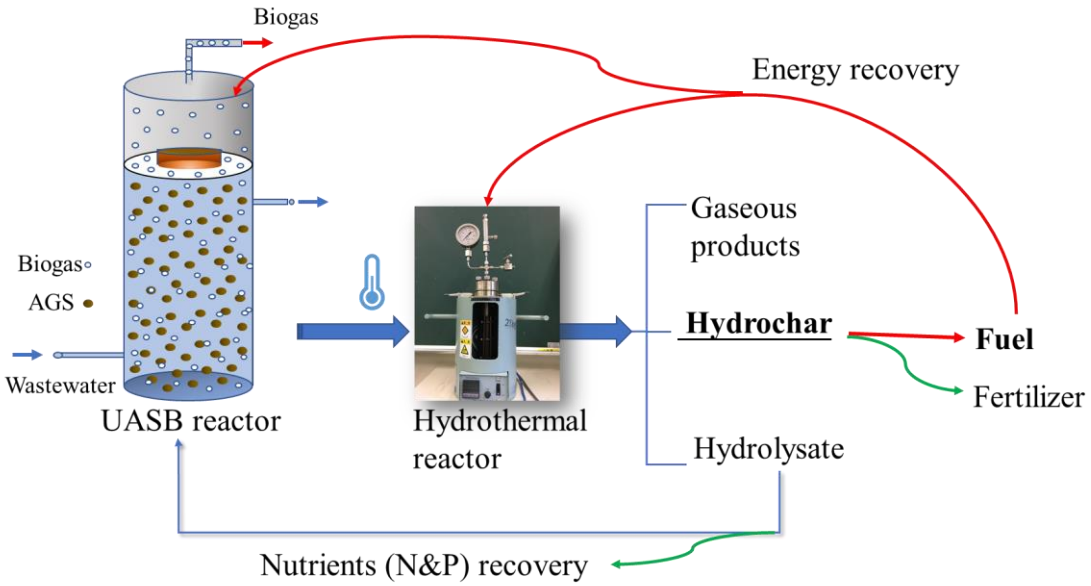

Fig.4-1 Energy and resources recovery based on the hybrid process coupling anaerobic granular sludge (AGS) wastewater treatment with hydrothermal carbonization (HTC) of AGS.

(a)

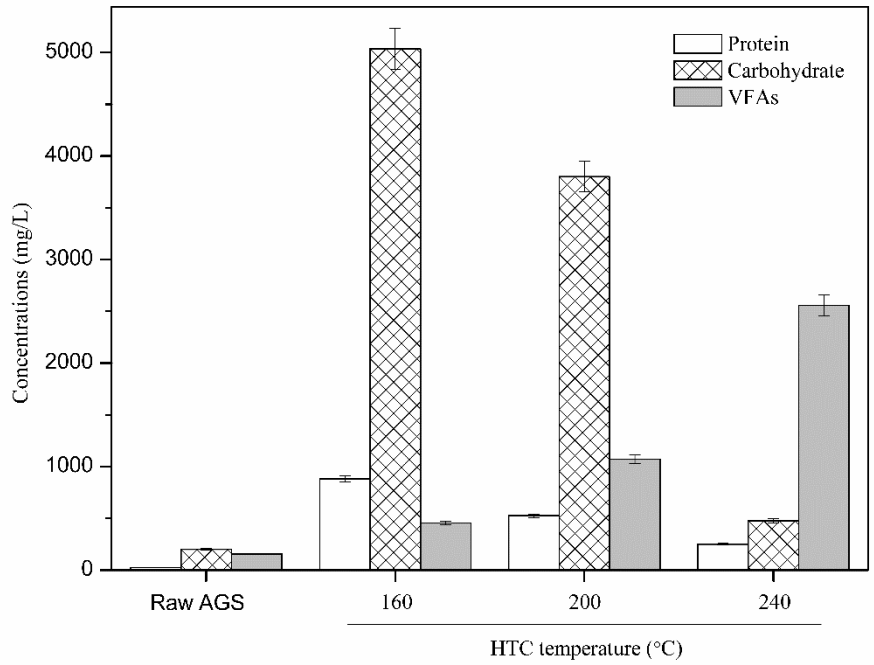

(b)

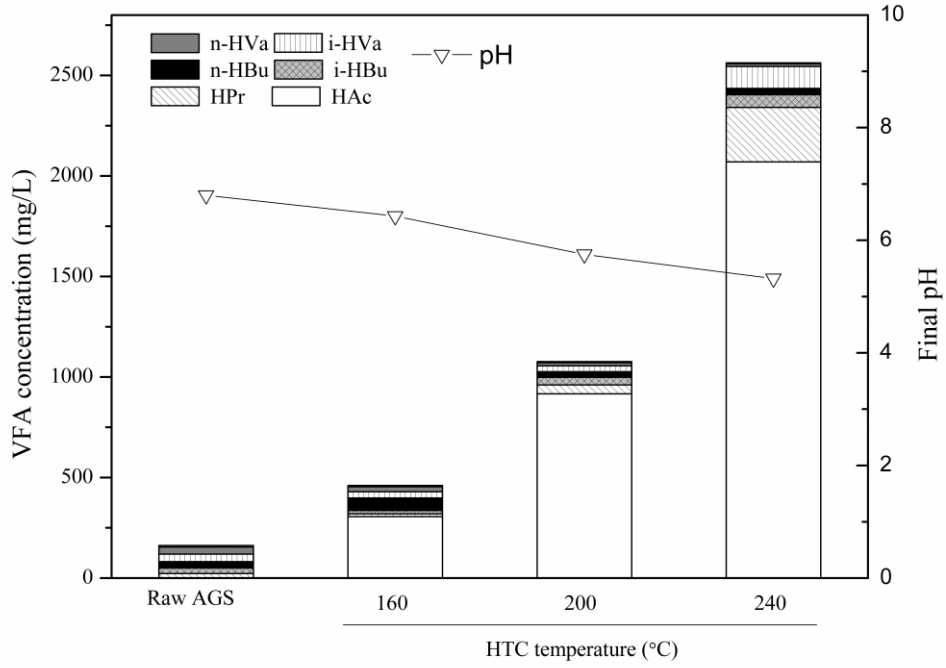

Fig.4-2 Variations of proteins, carbohydrates and VFAs released from AGS into the hydrolysate (a), and VFAs species and pH in the hydrolysate after HTT at different temperatures. Raw AGS denotes the concentrations in the supernatant.

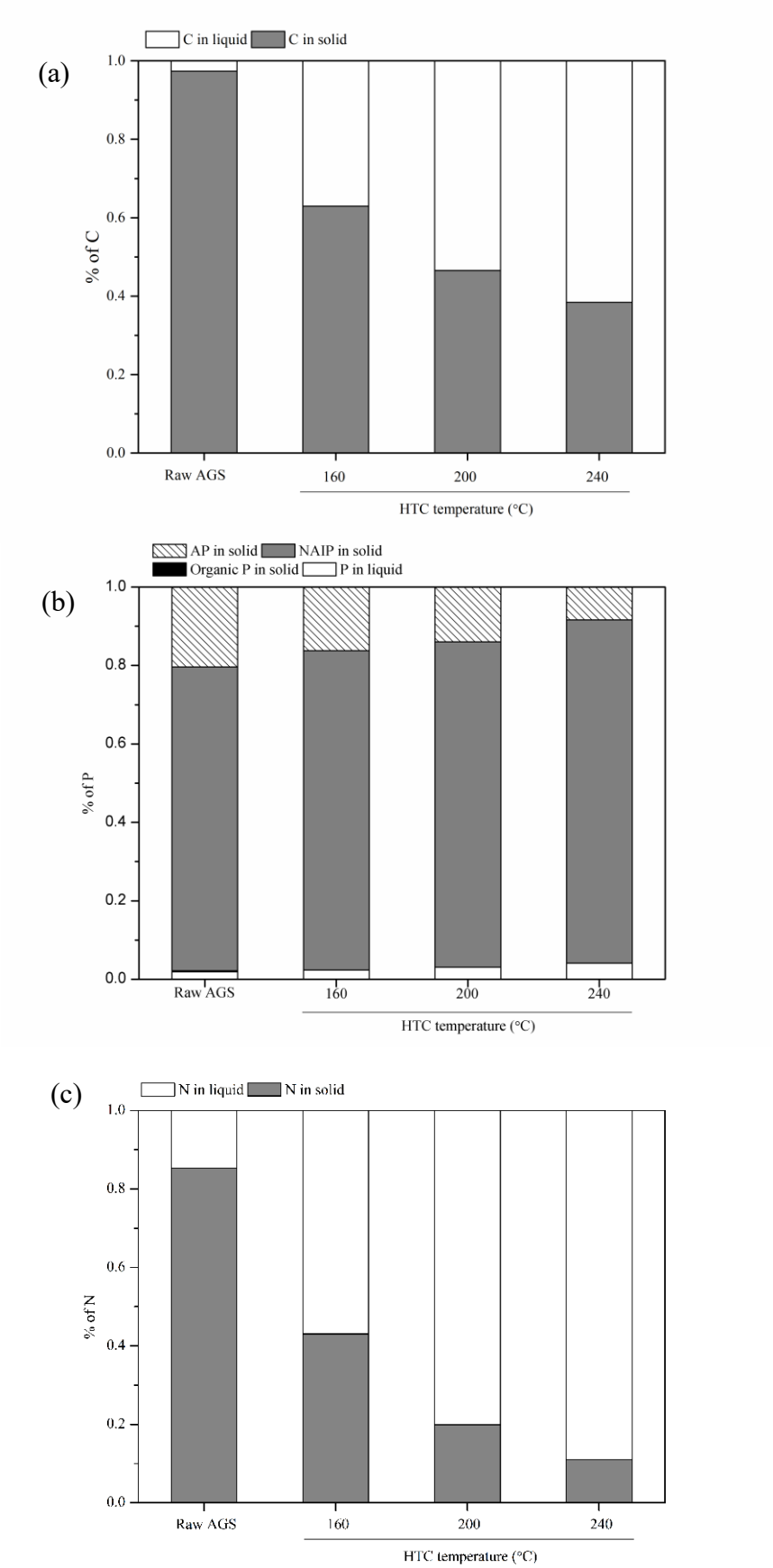

Fig.4-3 Changes of carbon (a), phosphorus (b) and nitrogen (c) distribution in the solid and liquid phases after HTT of AGS at different temperatures.

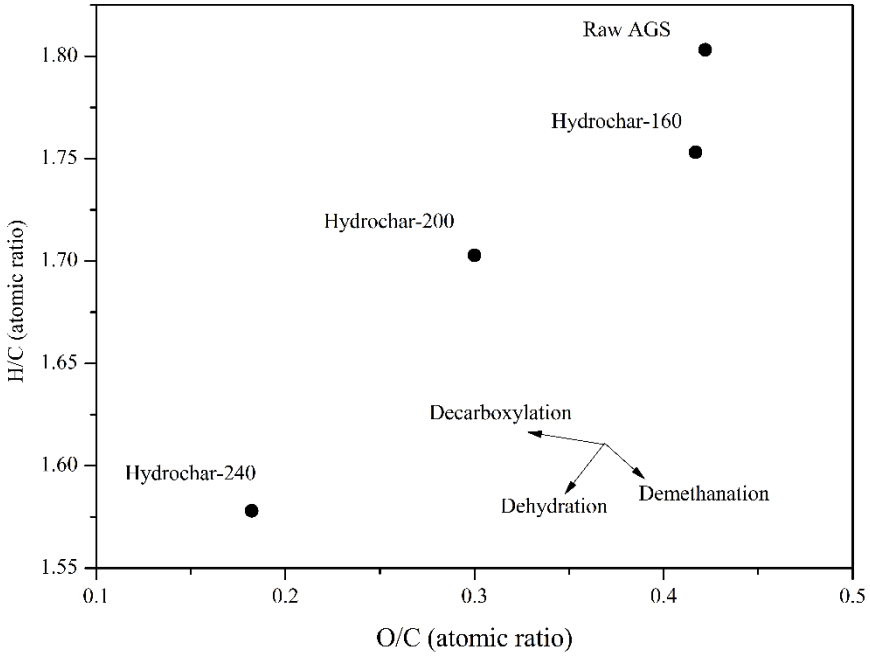

Fig.4-3 Atomic H/C versus O/C ratios (van Krevelen diagram) of the raw AGS and hydrochars produced at different HTT temperatures.

The arrows in the figure represent demethanation, dehydration, and decarboxylation pathways.

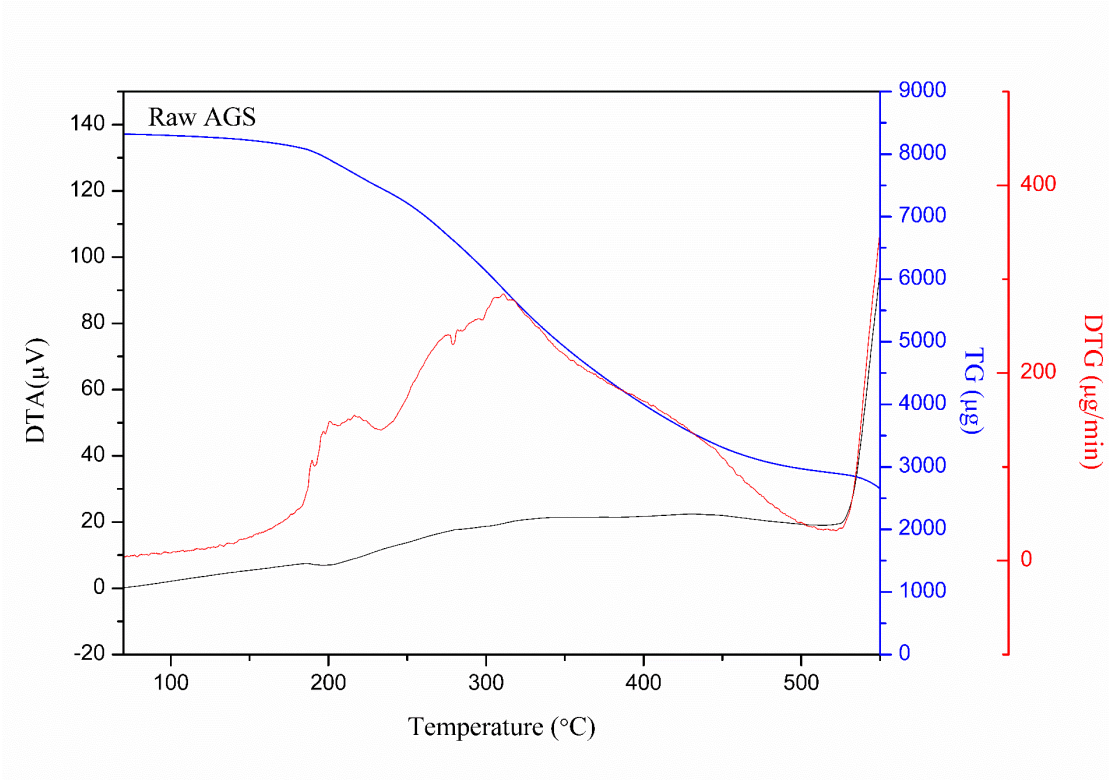
Raw AGS
DTA(μV)
TG (μg)
DTG (μg/min)
Temperature (°C)
140
120
100
80
60
40
20
0
-20
9000
8000
7000
6000
5000
4000
3000
2000
1000
0
400
200
0
100
200
300
400
500

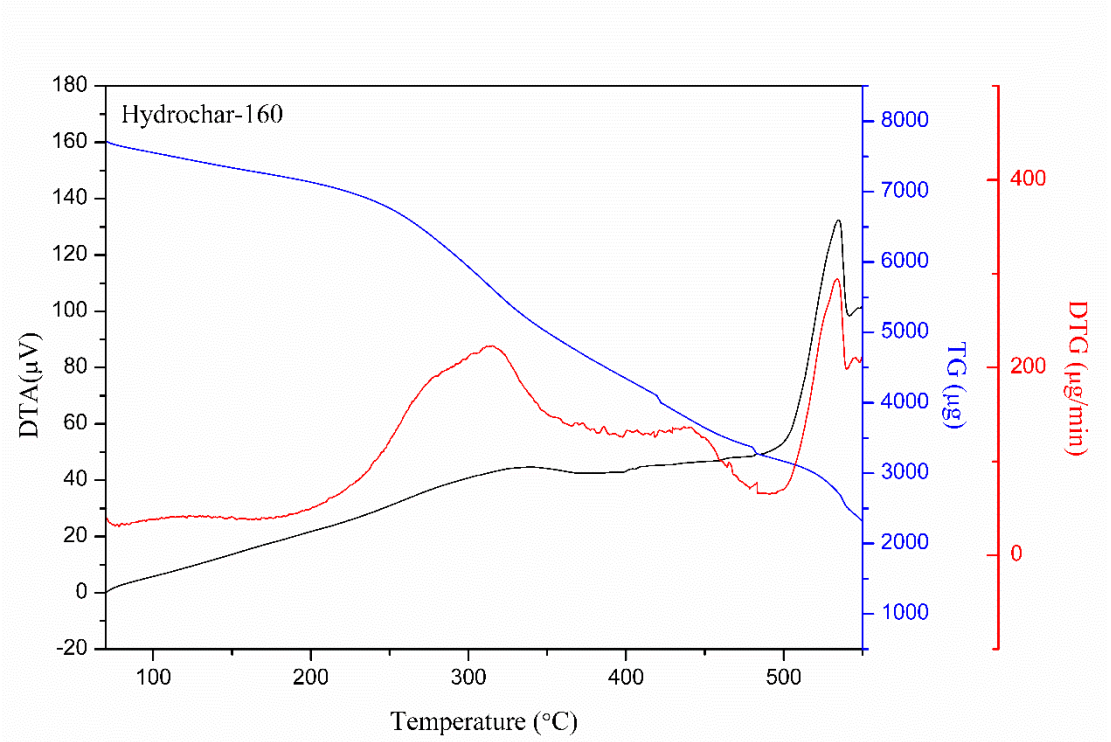
Hydrochar-160
DTA(μV)
TG (μg)
DTG (μg/min)
Temperature (°C)
180
160
140
120
100
80
60
40
20
0
-20
8000
7000
6000
5000
4000
3000
2000
1000
400
200
0
100
200
300
400
500

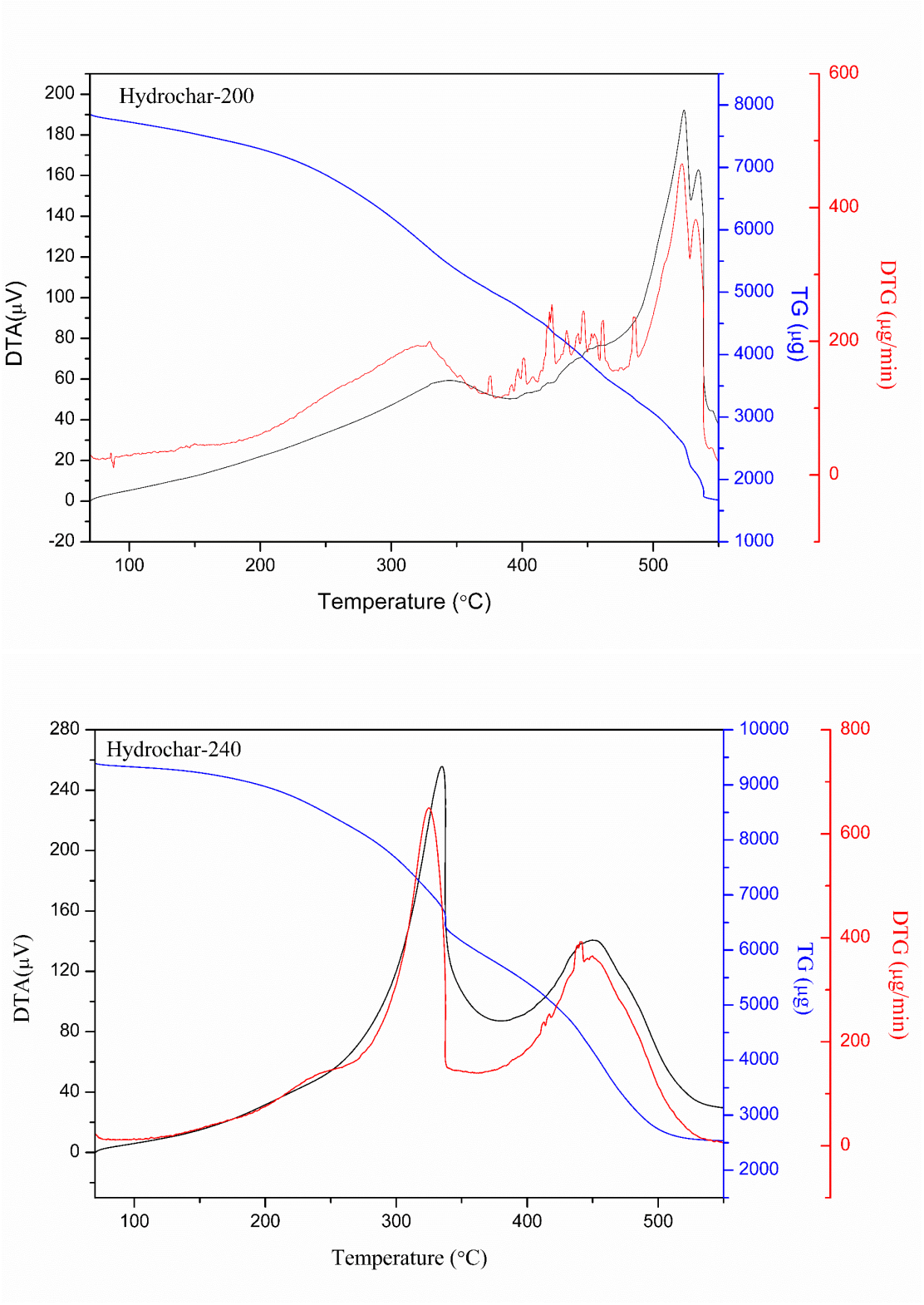

Fig.4-4 DTA/TG/DTG profiles for raw AGS and hydrochars produced at 160 ºC, 200 ºC and 240 ºC.

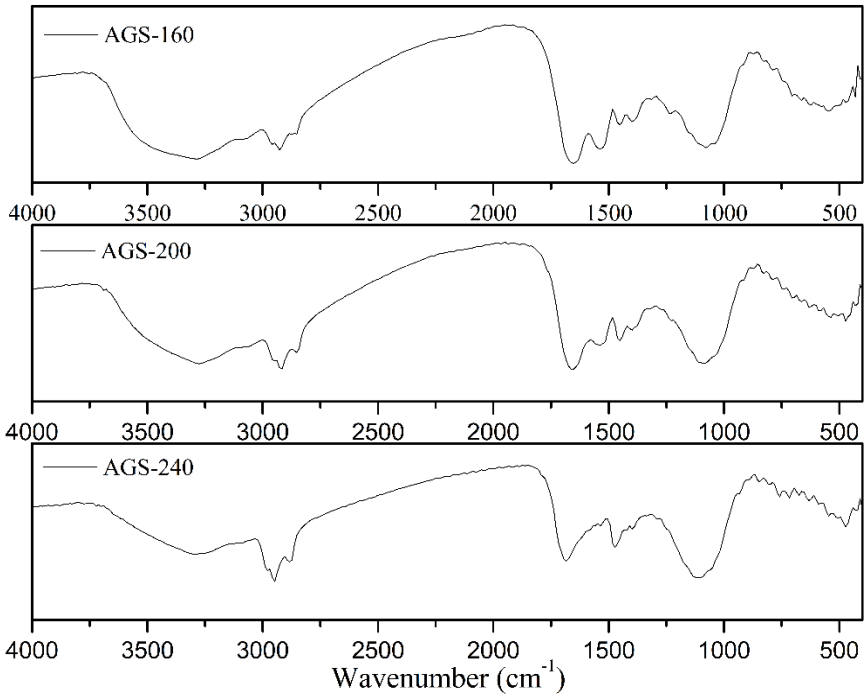

Fig.4-5 FTIR spectra of hydrochars at different hydrothermal temperature.

Chapter 5 Conclusions and future research

5.1 Conclusions

In this study, HTT of sewage sludge was investigated regarding the nutrients and energy recycle from wastewater. This study explored the effects of three macroelement cations (Fe, Ca and Al) in sewage sludge on P mobility and speciation in the resultant hydrochar by using HTC. And in order to dispose excess sewage sludge and recycle its nitrogen and phosphorus resources, hydrothermal pretreatment coupling with struvite crystallization was investigated. Hydrothermal pretreatment at different temperature and residence time were performed on sludge to maximize phosphate and ammonium release and their recovery from the resultant hydrolysate. At last, HTC of AGS was investigated at different temperatures (160 - 240 °C) regarding the distributions of C, N and P in the hydrothermal products to maximize the utilization efficiency of AGS. The detailed conclusions can be summarized as follows:

1. The effects of minerals on P transformation were studied during HTT of sludge. All the three metal ions (Fe, Al and Ca) demonstrated significant effects on P immobilization, among which Al was the most efficient effector, yielding 93% and 96% of P immobilization respectively at 5 and 10 mmol of Al mineral additives. Moreover, results from this study indicate that Al-P is the primary existing form in the hydrochar.
2. In the aspect of P fractionation, both Al and Fe rather than Ca promoted the formation of non-apatite inorganic phosphate (NAIP) and reduced the amount of apatite phosphate (AP) in the hydrochar. Whereas Ca addition contributed significantly to AP content.
3. A novel P recovery method from hydrothermal liquid (hydrolysate) was developed by using struvite precipitation. Struvite precipitation at initial pH 9 and Mg/P ratio of 1 was found to achieve the highest struvite containing precipitates with purity of 84.24% from the hydrolysate.
4. The hydrochar produced by HTC of AGS was evaluated at temperature between 160 and 240 ºC. The HHVs of hydrochar increased up to a maximum of 24 MJ/kg at 240 °C from 20 MJ/kg at 160 °C. The highest net energy output was about 6.86 MJ/kg achieved at 160 °C. In addition, the thermogravimetric analysis showed that the

combustion of the produced hydrochar could be completed in two phases rather than the one phase of the raw AGS.

5. HTC is also proved to be an effective method for P immobilization and recycle in AGS. The increase in HTC temperature exerted a limited effect on P distribution, resulting in less than 5% being released into the liquid. Most of P were immobilized into the produced hydrochar where the bioavailable P fractions > 80%.

5.2. Future research

Hydrothermal method is a promising technique for sewage sludge treatment and resource reclamation. Future works should focus on converting the sludge to functional materials with a view to making full use of the resources in sludge.

Biochar is recognized as an efficient material for carbon sequestration. And it can be used as soil conditioner achieving agricultural and environmental benefits. Besides, biochar shows promise as a potential low–cost sorbent for various contaminants. However, the sludge derived biochar has not been taken full advantage. In especial, AGS is very appropriate for biochar production due to its specific constitution. In the future research, in-depth modification of AGS based biochar is imperative as a renewable material for hazardous substance adsorption, such as heavy metals, antibiotics and all kinds of new type micropollutants. And more environmentally friendly and low-cost modification approaches need to be developed. As a result, a closed-loop wastewater treatment can be formed with the help of biochar production from sewage sludge.

References

APHA, 1998. Standard Methods for the Examination of Water and Wastewater. American Public Health Association, American Water Works Association, and Water Environment Federation, Washington, DC.

Berge, N.D., Ro, K.S., Mao, J., Flora, J.R., Chappell, M.A., Bae, S. 2011. Hydrothermal carbonization of municipal waste streams. Environ Sci Technol, 45(13), 5696-703.

Bougrier, C., Delgenès, J.P., Carrère, H., 2008. Effects of thermal treatments on five different waste activated sludge samples solubilisation, physical properties and anaerobic digestion. Chem Eng J., 139(2), 236-244.

Bruun, S., Harmer, S.L., Bekiaris, G., Christel, W., Zuin, L., Hu, Y., Jensen, L.S., Lombi, E. 2017. The effect of different pyrolysis temperatures on the speciation and availability in soil of P in biochar produced from the solid fraction of manure. Chemosphere, 169, 377-386.

Buchanan, J.R., Mote, C.R., Robinson, R.B. 1994. Thermodynamics of Struvite Formation. Transactions of the Asae, 37(2), 617-621.

Caravelli AH, Contreras EM, Zaritzky NE. 2010. Phosphorous removal in batch systems using ferric chloride in the presence of activated sludges. J. Hazard Mater, 177: 199-208.

Carlsson H, Aspegren H, Lee N, Hilmer A. 1997. Calcium phosphate precipitation in biological phosphorus removal systems. Water Res, 31: 1047-55.

Carpenter SR, Caraco NF, Correll DL, Howarth RW, Sharpley AN, Smith VH. Nonpoint pollution of surface waters with phosphorus and nitrogen. Ecol Appl, 1998; 8: 559-568.

Cheng, Y., Zheng, G., Wei, C., Mu, Q., Zheng, B., Wang, Z., Gao, M., Zhang, Q., He, K., Carmichael, G., Poschl, U., Su, H., 2016. Reactive nitrogen chemistry in aerosol water as a source of sulfate during haze events in China. Sci Adv, 2(12), e1601530.

Cordell D, Drangert JO, White S., 2009. The story of phosphorus: Global food security and food for thought. Global Environ Chang, 19: 292-305.

Dai L, Tan F, Wu B, He M, Wang W, Tang X, et al. 2015. Immobilization of phosphorus in cow manure during hydrothermal carbonization. J. Environ Manage, 157: 49-53.

Danso-Boateng, E., Holdich, R.G., Shama, G., Wheatley, A.D., Sohail, M., Martin, S.J. 2013. Kinetics of faecal biomass hydrothermal carbonisation for hydrochar production. Appl Energ, 111, 351-357.

Danso-Boateng, E., Shama, G., Wheatley, A.D., Martin, S.J., Holdich, R.G. 2015. Hydrothermal carbonisation of sewage sludge: effect of process conditions on product characteristics and methane production. Bioresour Technol, 177, 318-327.

Ding, L., Cheng, J., Qiao, D., Yue, L., Li, Y.Y., Zhou, J., Cen, K. 2017. Investigating hydrothermal pretreatment of food waste for two-stage fermentative hydrogen and methane co-production. Bioresour Technol, 241, 491-499.

Ekpo U, Ross AB, Camargo-Valero MA, Fletcher L.A. 2016. Influence of pH on hydrothermal treatment of swine manure: Impact on extraction of nitrogen and phosphorus in process water. Bioresour Technol, 214: 637-644.

Franca R, Samani TD, Bayade G, Yahia L, Sacher E. 2014. Nanoscale surface characterization of biphasic calcium phosphate, with comparisons to calcium hydroxyapatite and beta-tricalcium phosphate bioceramics. J. Colloid Interface Sci, 420: 182-188.

Frossard E, Bauer JP, Lothe F. 1997. Evidence of vivianite in FeSO4-flocculated sludges. Water Res, 31: 2449-2454.

Giusti, L., 2009. A review of waste management practices and their impact on human health. Waste Manag, 29(8), 2227-2239.

Goto, M., Nada, T., Kodama, A., Hirose, T. 1999. Kinetic Analysis for Destruction of Municipal Sewage Sludge and Alcohol Distillery Wastewater by Supercritical Water Oxidation. Ind Eng Chem Res, 38(5), 1863-1865.

He C, Wang K, Yang Y, Amaniampong PN, Wang JY. 2015. Effective nitrogen removal and recovery from dewatered sewage sludge using a novel integrated system of accelerated hydrothermal deamination and air stripping. Environ Sci Technol, 49, 6872-6880.

He, C., Giannis, A., Wang, J.Y. 2013. Conversion of sewage sludge to clean solid fuel using hydrothermal carbonization: Hydrochar fuel characteristics and combustion behavior. Appl Energ, 111, 257-266.

Hossain, M.K., Strezov, V., Chan, K.Y., Ziolkowski, A., Nelson, P.F. 2011. Influence of pyrolysis temperature on production and nutrient properties of wastewater sludge biochar. J. Environ Manage, 92(1), 223-228.

Huang R, Tang Y. 2016. Evolution of phosphorus complexation and mineralogy during (hydro)thermal treatments of activated and anaerobically digested sludge: Insights from sequential extraction and P K-edge XANES. Water Res, 100, 439-447.

Huang, R.X., Tang, Y.Z. 2015. Speciation Dynamics of Phosphorus during (Hydro)Thermal Treatments of Sewage Sludge. Environ Sci Technol, 49(24), 14466-14474.

Jain, A., Balasubramanian, R., Srinivasan, M.P. 2016. Hydrothermal conversion of biomass waste to activated carbon with high porosity: A review. Chem Eng J., 283, 789-805.

Kacprzak M, Neczaj E, Fijałkowski K, et al. 2017. Sewage sludge disposal strategies for sustainable development. Environ Res, 156: 39-46.

Karr, P.R., Keinath, T.M. 1978. Influence of particle size on sludge dewaterability. Journal (Water Pollution Control Federation), 1911-1930.

Khiari, B., Marias, F., Zagrouba, F., Vaxelaire, J. 2004. Analytical study of the pyrolysis process in a wastewater treatment pilot station. Desalination, 167(1-3), 39-47.

Kumar, S., Kothari, U., Kong, L., Lee, Y.Y., Gupta, R.B. 2011. Hydrothermal pretreatment of switchgrass and corn stover for production of ethanol and carbon microspheres. Biomass Bioenerg, 35(2), 956-968.

Li R, Zhang Z, Li Y, Teng W, Wang W, Yang T. 2015. Transformation of apatite phosphorus and non-apatite inorganic phosphorus during incineration of sewage sludge. Chemosphere, 141: 57-61.

Manara P, Zabaniotou A. 2012. Towards sewage sludge based biofuels via thermochemical conversion–a review. Renew Sust Energ Rev, 16: 2566-82.

Ministry of Housing and Urban-Rural Development of PRC (MOHURD) and National Development and Reform Commission (NDARC) Urban Sludge Treatment Technology Guide (2011) (in Chinese).

Mulchandani, A., Westerhoff, P. 2016. Recovery opportunities for metals and energy from sewage sludges. Bioresour Technol, 215, 215-26.

Ng, B. J., Zhou, J., Giannis, A., Chang, V. W. C., & Wang, J. Y. 2014. Environmental life cycle assessment of different domestic wastewater streams: policy effectiveness in a tropical urban environment. J. Environ Manage, 140, 60-68.

Ohlinger, K.N., Young, T.M., Schroeder, E.D. 1998. Predicting struvite formation in digestion. Water Res, 32(12), 3607-3614.

Oliveira, I., Blohse, D., Ramke, H.G. 2013. Hydrothermal carbonization of agricultural residues. Bioresour Technol, 142, 138-146.

Peccia, J., Westerhoff, P., 2015. We should expect more out of our sewage sludge. Environ. Sci. Technol, 49(14), 8271-8276.

Peterson, A.A., Vogel, F., Lachance, R.P., Froling, M., Antal, M.J., Tester, J.W. 2008. Thermochemical biofuel production in hydrothermal media: A review of sub- and supercritical water technologies. Energy Environ. Sci, 1(1), 32-65.

Qian TT, Jiang H. Migration of Phosphorus in Sewage Sludge during Different Thermal Treatment Processes. Acs Sustain Chem Eng, 2014; 2: 1411-1419.

Rahaman, M.S., Mavinic, D.S., Meikleham, A., Ellis, N. 2014. Modeling phosphorus removal and recovery from anaerobic digester supernatant through struvite crystallization in a fluidized bed reactor. Water Res, 51, 1-10.

Rittmann, B.E., Mayer, B., Westerhoff, P., Edwards, M. 2011. Capturing the lost phosphorus. Chemosphere, 84(6), 846-853.

Ruban V, Lopez-Sanchez JF, Pardo P, Rauret G, Muntau H. 1999. Quevauviller P. Selection and evaluation of sequential extraction procedures for the determination of phosphorus forms in lake sediment. J Environ Monit; 1: 51-56.

Ruyter, H.P. 1982. Coalification model. Fuel, 61(12), 1182-1187.

Shanableh, A., Jomaa, S. 2001. Production and transformation of volatile fatty acids from sludge subjected to hydrothermal treatment. Water Sci Technol, 44(10), 129-135.

Singh, K.P., Mohan, D., Sinha, S., Dalwani, R. 2004. Impact assessment of treated/untreated wastewater toxicants discharged by sewage treatment plants on health, agricultural, and environmental quality in the wastewater disposal area. Chemosphere, 55(2), 227-255.

Smith S, Takacs I, Murthy S, Daigger G, Szabo A. 2008. Phosphate complexation model and its implications for chemical phosphorus removal. Water Environ Res, 80: 428-438.

Steen I. 1998. Phosphorus availability in the 21st century: Management of a nonrenewable resource. Phosphorus Potassium, 217: 25-31.

Stevenson FJ, Goh KM. Infrared Spectra of Humic Acids and Related Substances. Geochim Cosmochim Ac 1971; 35: 471-483.

Stratful, I., Scrimshaw, M.D., Lester, J.N. 2001. Conditions influencing the precipitation of magnesium ammonium phosphate. Water Res, 35(17), 4191-4199.

Tchobanoglous, G., Burton, F.L., Stensel, H.D., 2003. Wastewater Engineering: Treatment and Reuse(4th Edition). Boston: McGraw-Hill.

Tilman D, Fargione J, Wolff B, D'Antonio C, Dobson A, Howarth R, et al. 2001. Forecasting agriculturally driven global environmental change. Science, 292: 281-284.

Toufiq Reza, M., Freitas, A., Yang, X., Hiibel, S., Lin, H., Coronella, C.J. 2016. Hydrothermal carbonization (HTT) of cow manure: Carbon and nitrogen distributions in HTT products. Environ Prog Sustain Energy, 35(4), 1002-1011.

Tsang, K., Vesilind, P. 1990. Moisture distribution in sludges. Water Sci. Technol, 22(12), 135-142.

Tyagi, V.K., Lo, S.-L. 2013. Sludge: A waste or renewable source for energy and resources recovery? Renew Sust Energ Rev, 25, 708-728.

US EPA. 1995. Process design manual: land application of sewage sludge and domestic Septage, 625/R-95/001. Washington, DC.

Valdez, P.J., Nelson, M.C., Wang, H.Y., Lin, X. N., Savage, P.E., 2012. Hydrothermal liquefaction of Nannochloropsis sp.: Systematic study of process variables and analysis of the product fractions. Biomass Bioenerg, 46, 317-331.

Wang L, Li A. 2015. Hydrothermal treatment coupled with mechanical expression at increased temperature for excess sludge dewatering: The dewatering performance and the characteristics of products. Water Res, 68: 291-303.

Wang T, Zhai Y, Zhu Y, Peng C, Wang T, Xu B, et al. 2017. Feedwater pH affects phosphorus transformation during hydrothermal carbonization of sewage sludge. Bioresour Technol, 245: 182-187.

Wang W, Luo Y, Qiao W. 2009. Possible solutions for sludge dewatering in China. Front Env Sci Eng, 4:102-107.

Wang, X., Qiu, Z., Lu, S., Ying, W. 2010. Characteristics of organic, nitrogen and phosphorus species released from ultrasonic treatment of waste activated sludge. J. Hazard Mater, 176(1), 35-40.

Wilfert P, Kumar PS, Korving L, Witkamp GJ, van Loosdrecht MC. 2015. The relevance of phosphorus and iron chemistry to the recovery of phosphorus from wastewater: A Review. Environ Sci Technol, 49: 9400-14.

Wilson, C.A., Novak, J.T. 2009. Hydrolysis of macromolecular components of primary and secondary wastewater sludge by thermal hydrolytic pretreatment. Water Res, 43(18), 4489-4498.

Wu H, Ikeda-Ohno A, Wang Y, Waite TD. 2015. Iron and phosphorus speciation in Fe-conditioned membrane bioreactor activated sludge. Water Res, 76: 213-226.

Xu, H., He, P., Wang, G., Shao, L., Lee, D. 2011. Anaerobic storage as a pretreatment for enhanced biodegradability of dewatered sewage sludge. Bioresour Technol, 102(2), 667-71.

Yang Y, Zhao YQ, Babatunde AO, Wang L, Ren YX, Han Y. 2006. Characteristics and mechanisms of phosphate adsorption on dewatered alum sludge. Sep Purif Technol, 51, 193-200.

Yu, Y., Lou, X., Wu, H., 2008. Some recent advances in hydrolysis of biomass in hot compressed water and its comparisons with other hydrolysis methods. Energy Fuel, 22 (1), 46–60.

Zhang, Q.H., Yang, W.N., Ngo, H.H., Guo, W.S., Jin, P.K., Dzakpasu, M., Yang, S.J., Wang, Q., Wang, X.C., Ao, D. 2016. Current status of urban wastewater treatment plants in China. Environ Int, 92-93, 11-22.

Acknowledgments

First of all, I would like to thank my supervisor, Prof. Zhenya Zhang, for all his support. He gave me so much support during these three years. I do feel lucky to have a tolerant and generous person help me through my research. I would also like to thank Prof. Zhongfang Lei. She also gave me a great help with my research. Her staidness and persistence to research teach me a lot.

Secondly, special thanks should go to my thesis committee members, Prof. Zhenya Zhang, Prof. Kaiqin Xu, Prof. Zhongfang Lei, and Prof. Kazuya Shimizu for their patient reading and listening, valuable suggestions and comments. All the instructors provided great help for the improvement of my dissertation and future study. The inputs and recommendations for changes and improvements to the thesis are appreciated.

Furthermore, I would like to thank the China Scholarship Council (CSC) for financially supporting my oversea study.

I also want to say thank you to all the members of our lab, which have brought me entertainment and helped me a lot.

At last, I want to thank my parents and my wife, Dr. Xi Yang, who always give me all the support and love that I need.